Bioorganic Chemistry 89 (2019) 103027

Contents lists available at ScienceDirect

Bioorganic Chemistry

journal homepage: www.elsevier.com/locate/bioorg

Novel chromanone-dithiocarbamate hybrids as multifunctional AChE inhibitors with β-amyloid anti-aggregation properties for the treatment of Alzheimer's disease

Neng Jiang[a,b,1], Jiaoli Ding[a,1], Jing Liu[c], Xiaona Sun[b], Zhipeng Zhang[a], Zhongxia Mo[b], Xiao Li[b], Hong Yin[e], Weizhong Tang[d,*], Sai-Sai Xie[a,**]

[a] National Pharmaceutical Engineering Center for Solid Preparation in Chinese Herbal Medicine, Jiangxi University of Traditional Chinese Medicine, Nanchang, PR China
[b] Department of Pharmacy, Affiliated Tumor Hospital of Guangxi Medical University, Nanning, PR China
[c] School of Pharmacy, Jiangxi University of Traditional Chinese Medicine, Nanchang, PR China
[d] Department of Gastrointestinal Surgery, Affiliated Tumor Hospital of Guangxi Medical University, Nanning, PR China
[e] College of Chemistry & Pharmacy, Northwest A&F University, Yangling, PR China

ARTICLE INFO

Keywords:
Alzheimer's disease
Chromanone
Dithiocarbamate
Acetylcholinesterase
Multifunctional agent

ABSTRACT

By connecting chromanone with dithiocarbamate moieties through flexible linkers, a series of hybrids as novel multifunctional AChE inhibitors have been designed and synthesized. Most of these compounds displayed strong and excellently selective inhibition to eeAChE as well as potent inhibition to self- and AChE-induced Aβ aggregation. Among them, compound **6c** showed the best activity to inhibit eeAChE (IC_{50} = 0.10 μM) and AChE-induced Aβ aggregation (33.02% at 100 μM), and could effectively inhibit self-induced Aβ aggregation (38.25% at 25 μM). Kinetic analysis and docking study indicated that compound **6c** could target both the CAS and PAS, suggesting that it was a dual binding site inhibitor for AChE. Besides, it exhibited good ability to penetrate the BBB and low neurotoxicity in SH-SY5Y cells. More importantly, compound **6c** was well tolerated in mice (2500 mg/kg, po) and could attenuate the memory impairment in a scopolamine-induced mouse model. Overall, these results highlight **6c** as a promising multifunctional agent for treating AD and also demonstrate that the dithiocarbamate is a valid scaffold for design of multifunctional AChE inhibitors.

1. Introduction

Alzheimer's disease (AD) is a complex neurodegenerative disease that leads to severe menace to human health characterized by memory loss, cognitive deficits and behavioral abnormalities [1]. Many AD patients lack daily self-care ability and need long term home care, which increases patients' family burden and influences the development of the society to a great extent. The reports from the Alzheimer's Association indicate that the number of AD patients is now nearly 47 million and the number is projected to increase to 100 million by 2050 all over the world [2]. The fast-growing population of AD patients is considered to be severe and urgent health issue for society.

It has been more than one hundred years since the first report about AD. However, the etiopathogenesis of AD is still unclear, and the AD treatment remains a challenge for the pharmaceutical community. Many factors and targets including deficits of acetylcholine (ACh), amyloid-β (Aβ) peptide deposits and hyperphosphorylated tau protein, etc. are regarded to be associated with the initiation and development of AD [3]. Over the past few decades, a lot of academic institutions and pharmaceutical companies make great efforts to develop novel chemical molecular and biological medicines for the treatment of AD. Unfortunately, most of these clinical trial anti-AD drugs have been ended up with failure [4,5]. To date, the current clinical treatment of AD mainly relies on the cholinergic hypothesis [6,7]. This hypothesis asserts that the decline of ACh levels in brain leads to memory and cognitive impairments of AD patient, and inhibiting the ACh metabolism can improve the ACh level, which alleviate these symptoms. Based on this notion, four of the five drugs approved by the FDA are cholinesterase inhibitors (Tacrine, Donepezil, Galantamine and Rivastigmine) (Fig. 1).

* Corresponding author.
** Corresponding author.
E-mail addresses: tangweizhong@gxmu.edu.cn (W. Tang), xiesaisainanchang@hotmail.com (S.-S. Xie).
[1] These authors contributed equally to this work.

https://doi.org/10.1016/j.bioorg.2019.103027
Received 22 April 2019; Received in revised form 30 May 2019; Accepted 30 May 2019
Available online 31 May 2019

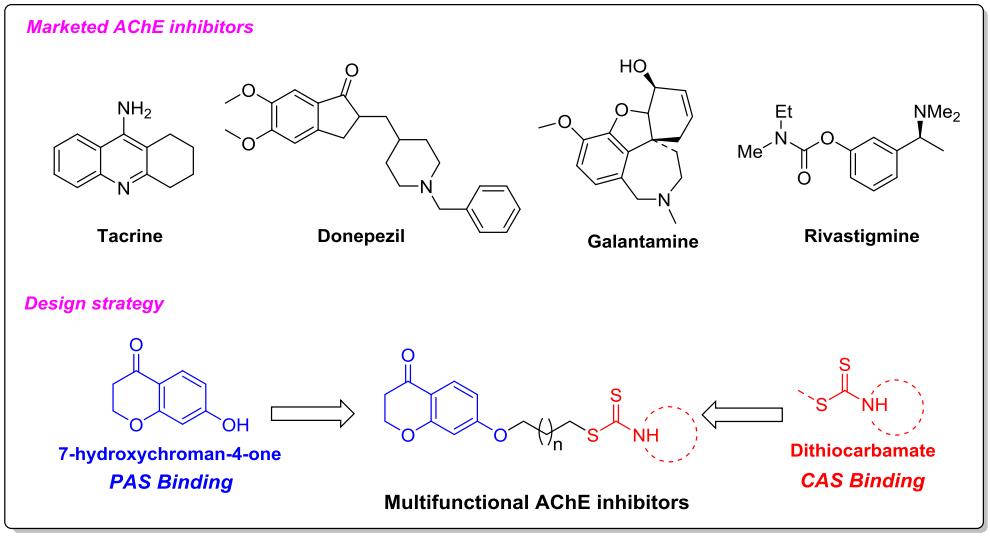

Fig. 1. Marketed AChE inhibitors for the treatment of AD and design strategy for chromanone-dithiocarbamate hybrids.

Acetylcholinesterase (AChE) and butyrylcholinesterase (BuChE) are two types of cholinesterases that can break down ACh in the central nervous system (CNS) [8]. However, in contrast to AChE, the pathological mechanism of BuChE in AD is not yet completely identified. Although a few studies suggest that BuChE may be also beneficial to AD treatment, BuChE mainly distributes in peripheral tissues, so the inhibition of BuChE may cause adverse effects in the peripheral system [9]. For instance, tacrine, one of the first drugs approved for AD treatment with both inhibitory activities of AChE and BuChE, was withdrawn due to the serious hepatotoxicity and other side-effect in the peripheral system [10,11]. Therefore, development of selective AChE inhibitors is the more promising approach for AD treatment. The crystallographic structure of AChE shows that the enzyme has two binding active sites, which are connected by a nearly 20 Å deep narrow gorge. The two binding active sites are a peripheral anionic site (PAS) near the entry of the gorge and a catalytic active site (CAS) at the bottom of the gorge [12]. Studies show that the structural features of AChE inhibitors should contain three parts: a CAS binding moiety, a PAS binding moiety and a linker between these two moieties to fulfil the structural requirements of AChE [13].

Apart from the cholinergic hypothesis, another hypothesis called the amyloid cascade hypothesis suggests that Aβ peptide is also a causative factor in the course of AD pathology [14,15]. Aβ peptide consists of 39–43 amino acid residues, which is a proteolytic product of the amyloid precursor protein (APP). Biochemical studies reveal that the Aβ peptides can form monomers, oligomers and large Aβ plaques, which are toxic to neuronal and mitochondrial functions, ultimately leading to neurodegeneration and cognitive dysfunction [16]. $Aβ_{1-40}$ and $Aβ_{1-42}$ are the two main isoforms of Aβ peptides. However, the latter is more prone to aggregate into fibrils and more toxic to neuronal cells than the former [17]. Thus, inhibition of $Aβ_{1-42}$ aggregation seems to be also important for AD treatment.

In fact, recent studies indicate that there is a close relationship between AChE and Aβ aggregation. The AChE can promote Aβ aggregation and amyloid fibril formation through its PAS [18,19]. The interaction of Aβ and the PAS of AChE produces stable AChE-Aβ complexes, and the complexes are more toxic than Aβ peptide aggregates. Thus, developing dual binding site inhibitors, which can bind simultaneously to the CAS and PAS of AChE, appears to be a very promising strategy for AD treatment, because they can not only improve cognition by inhibiting AChE, but also slow the Aβ aggregation contribute to AD pathogenesis [20].

Dithiocarbamate is a versatile pharmacophore in drug design, which has been attracting considerable interest due to their diverse activities. The reported biological activities of dithiocarbamate derivatives include anti-cancer, anti-bacteria and carbonic anhydrase inhibition, etc. [21–23]. However, compounds containing a dithiocarbamate moiety were rarely reported to treat neurodegenerative disease, such as AD. Recently, our group found that some dithiocarbamate derivatives could inhibit AChE through the interactions between their dithiocarbamate moieties and the CAS of AChE, and several of them also showed potential ability to inhibit self-induced Aβ aggregation [24,25]. Therefore, our recent research interests mainly focus on developing dithiocarbamate derivatives as new AChE inhibitors with additional Aβ anti-aggregation properties for the treatment of AD. Chromanones, a group of naturally occurring compounds, are ubiquitous in nature, especially in plants [26]. Recent years, they received much attention due to their wide use in designing compounds for the treatment of AD. Some chromanone derivatives have been demonstrated to possess potent AChE inhibitory activity, and the molecular docking studies suggest that chromanone moiety can exert AChE inhibitory effect through interacting with the PAS of AChE [27,28].

In light of the potential roles of dithiocarbamate and chromanone moieties mentioned above in design of AChE inhibitors, in present work, our group attempted to connect these two moieties by a flexible linker to produce a series of new chromanone-dithiocarbamate hybrids as multifunctional AChE inhibitors for AD treatment (Fig. 1). All designed compounds were evaluated in vitro to determine their ability to inhibit AChE. The compounds with good AChE inhibitory activity and BBB permeability were also tested to inhibit self- and AChE -induced Aβ aggregation. Finally, the most promising compound fished out from the above assays was selected for further studies including kinetic and molecular modeling analysis of its binding mode with AChE, acute toxicity, cytotoxicity in SH-SY5Y neuroblastoma cells and the neuroprotective effects on scopolamine-induced cognitive impairment in mice.

2. Results and discussion

2.1. Chemistry

The syntheses of the target compounds are depicted in Scheme 1. The commercially available resorcinol was reacted with 3-chloropropionic acid in the presence of trifluoromethanesulphonic acid to obtain the intermediate **3**, which was then cyclized in aqueous NaOH to produce 7-hydroxychroman-4-one (**4**). Reaction of compound **4** with corresponding α, ω-dibromoalkanes using K_2CO_3 in acetone provided intermediates **5a-d**. Finally, following our previously reported method

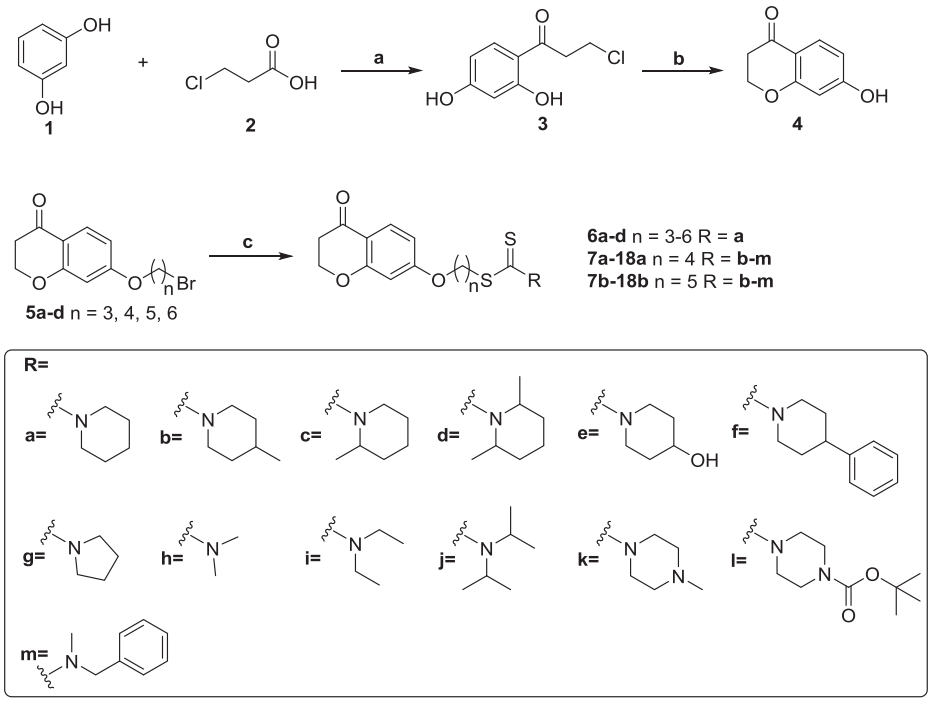

Scheme 1. Synthesis of the target compounds **6–18**. Reagents and conditions: (**a**) 3-chloropropanoic acid, CF_3SO_3H, 80 °C, 30 min; (**b**) 2 M NaOH (aq), 5 °C to r.t., 6 M H_2SO_4 (aq), 2 h. (**c**) α, ω-dibromoalkanes, K_2CO_3, acetone, reflux, 4 h; (**d**) appropriate secondary amines, CS_2, TEA, DMF, r.t., 12 h.

[24], the target compounds **6-18** were accomplished in good yields by reacting compounds **5a-d** with the CS_2, appropriate secondary amines and TEA in DMF.

2.2. In vitro eeAChE and eqBuChE inhibition studies

The inhibitory activities of the target compounds **6-18** against electric eel acetylcholinesterase (eeAChE) and equine serum butyrylcholinesterase (eqBuChE) were evaluated by the Ellman's method. For comparison purposes, the marketed drugs, donepezil and tacrine, were taken as reference compounds [29]. The inhibition data are reported in Table 1 as IC_{50} (μM) or, for poorly active compounds, as the percentage of inhibition at 10 μM. It can be seen from the table that all compounds exhibit very weak or inactive inhibitory activity for eqBuChE, which suggest that our present compounds are obviously selective inhibitors to eeAChE. Of these compounds, compounds **6b** and **6c** exhibited the most potent inhibitory activity for eeAChE, showing IC_{50} values of 0.12 and 0.10 μM, respectively, which were 4.5 times stronger than that of tacrine.

According to the previous studies, the linker length between the CAS and PAS binding moieties plays a crucial role in AChE inhibition [30,31]. Therefore, to determine the optimal length in present study, compounds **6a-d** with linker length ranging from three to six carbon atoms (n = 3–6) were prepared in our initial step. Biological evaluation indicated that compounds **6b** and **6c** presented more potent inhibitory activities than other compounds, which suggested that the linkers containing four or five carbon atoms seemed to be suitable for eeAChE inhibition.

After obtaining the optimal linker length, we next introduced different substituents to the terminal group for exploring the SARs. As shown in the Table 1, introduction of a methyl substituent to piperidine ring gave rise to a decrease in inhibiting eeAChE. All compounds **7-9** bearing mono- or di-methyl substituents on piperidine ring showed lower inhibitory activity than their no methyl analogues **6b** and **6c**. However, the position of the methyl group on piperidine ring influenced the activity in different degree. The position 4 seemed to be essential for the inhibitory activity. When it was substituted by the methyl group, compounds **7a** and **7b** displayed a large drop in eeAChE inhibition, especially for compound **7b**, which contain a five-carbon atom linker, showed a poor inhibitory activity, which was less than 50% at 10 μM. In addition, a hydroxy group or a bulky group on this position of piperidine ring was also not favorable for the inhibitory activity, as compounds **10a-b** possessing a hydroxy group and compounds **11a-b** having a phenyl group exhibited a total loss activity on eeAChE inhibition.

In order to further explore the SARs, the effects on replacing the piperidine group with other secondary amines were also investigated. When the piperidine ring was contracted to a pyrrole ring, the inhibitory activity was significantly reduced, as compounds **12a** and **12b** only provided a micromolar inhibition for eeAChE. Moreover, the inhibitory activities of compounds **13-15** substituted with alkyl amines were continuously improved with gradually increasing the alkyl groups. Compounds **15a-b** with a diisopropylamine group presented more potent inhibitory activity than its counterparts **13a-b** and **14a-b**. Finally, replacement of the piperidine with 4-substituted piperizine or with a *N*-methylbenzylamine could not improve the inhibitory activity, as compounds **16-18** did not give any inhibition for eeAChE.

2.3. Kinetic study of eeAChE inhibition

To gain insight into the inhibition mode of the present compound for eeAChE, compound **6c** with the most potent activity for eeAChE inhibition was selected for kinetic study. It can be seen from the Fig. 2 that the Lineweaver-Burk reciprocal plots show both increased slopes (decreased V_{max}) and intercepts (higher K_m) at increasing concentration of the inhibitor, which indicated a mixed-type inhibition. These results implied that compound **6c** might be a dual binding site AChE inhibitor, which could target the catalytic active site (CAS) and the peripheral anionic site (PAS) of AChE simultaneously.

2.4. Molecular modeling studies of AChE

To further confirm the binding mode of compound **6c** with AChE, docking studies were performed using a Molecular Operating

Table 1
Inhibition of eeAChE and eqBuChE by compounds **6–18**.

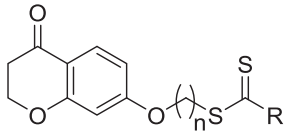

Compd.	n	R	eeAChE[a] IC_{50}(μM)/Inhibition (%)	eqBuChE Inhibition (%)[b]
6a	3	**a**	0.37 ± 0.07	15.03 ± 3.32
6b	4	**a**	0.12 ± 0.01	16.26 ± 2.45
6c	5	**a**	0.10 ± 0.03	14.38 ± 7.63
6d	6	**a**	0.92 ± 0.26	7.67 ± 1.21
7a	4	**b**	3.99 ± 1.09	14.15 ± 2.46
7b	5	**b**	45.43 ± 8.79%	21.37 ± 10.05
8a	4	**c**	0.24 ± 0.04	n.a.[c]
8b	5	**c**	0.23 ± 0.03	18.93 ± 6.17
9a	4	**d**	0.59 ± 0.12	n.a.[c]
9b	5	**d**	0.54 ± 0.11	5.18 ± 1.03
10a	4	**e**	19.25 ± 2.68%	23.02 ± 9.84
10b	5	**e**	32.21 ± 9.15%	24.73 ± 4.51
11a	4	**f**	12.00 ± 4.05%	13.84 ± 5.67
11b	5	**f**	26.22 ± 6.34%	n.a.[c]
12a	4	**g**	5.11 ± 0.99	21.92 ± 8.72
12b	5	**g**	3.02 ± 0.75	9.97 ± 1.06
13a	4	**h**	35.40 ± 3.64%	8.79 ± 1.14
13b	5	**h**	44.04 ± 10.20%	12.73 ± 5.13
14a	4	**i**	1.63 ± 0.78	6.19 ± 2.68
14b	5	**i**	0.94 ± 0.13	10.11 ± 1.42
15a	4	**j**	1.16 ± 0.51	5.67 ± 0.96
15b	5	**j**	0.51 ± 0.04	21.37 ± 11.35
16a	4	**k**	18.16 ± 2.57%	n.a.[c]
16b	5	**k**	13.74 ± 3.56%	8.49 ± 2.61
17a	4	**l**	13.20 ± 3.61%	5.79 ± 1.49
17b	5	**l**	23.15 ± 8.78%	11.53 ± 3.44
18a	4	**m**	10.15 ± 3.43%	n.a.[c]
18b	5	**m**	10.32 ± 5.12%	n.a.[c]
Donepezil	–	–	0.042 ± 0.005	IC_{50} = 4.12 ± 0.87 μM
Tacrine	–	–	0.45 ± 0.03	IC_{50} = 0.026 ± 0.002 μM

[a] The 50% inhibitory concentration of eeAChE or percent inhibition with inhibitor at 10 μM (means ± SD of three experiments).
[b] The percent inhibition of eqBuChE with inhibitor at 10 μM (means ± SD of three experiments).
[c] n. a. = no active. Compounds defined "no active" means that percent inhibition is less than 5.0% at a concentration of 10 μM in the assay conditions.

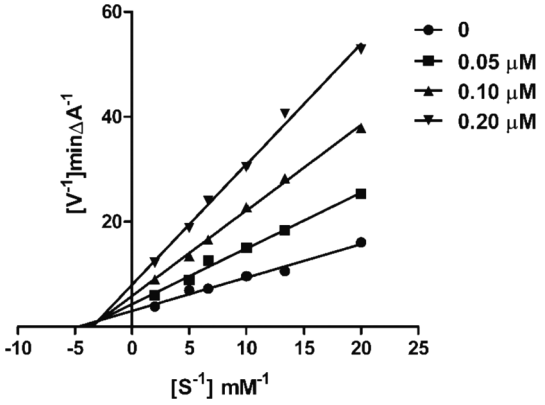

Fig. 2. Kinetic study on the mechanism of eeAChE inhibition by compound **6c**. Overlaid Lineweaver-Burk reciprocal plots of eeAChE initial velocity at increasing substrate concentration (0.05–0.50 mM) in the absence of inhibitor and in the presence of **6c** are shown. Lines were derived from a weighted least-squares analysis of the data points.

Environment (MOE 2015.10) software package. The structure of *Tc*AChE co-crystallized with donepezil (PDB code 1EVE) was used to establish the starting model of AChE. As shown in the Fig. 3, compound **6c** fits well in the active site of AChE, which can occupy the entire enzymatic CAS, mid-gorge site and PAS. The chromanone moiety located at the PAS of the enzyme, forming a π-π stacking interaction with the indole ring of Trp 279 (3.48 Å). Similar to our previous result [24,25], the piperidinyldithiocarbamate moiety of compound **6c** was bound to the CAS through hydrophobic interactions with residues Trp 84, Asn 85, Ser122 and Gln 69. Moreover, the polymethylene chain was folded in a conformation in the mid-gorge, which allowed it to establish hydrophobic interactions with Phe330 and Tyr 334. All in all, this docking study demonstrated that compound **6c** was a dual binding site inhibitor of AChE, which was in agreement with our result from kinetic analysis.

2.5. Blood-brain barrier (BBB) permeation assay

The ability to cross the blood-brain barrier (BBB) is a crucial factor for successful CNS drugs [32]. Thus, we performed a parallel artificial membrane permeation assay of blood-brain barrier (PAMPA-BBB) to investigate whether the present compounds could penetrate the BBB. This assay stablished by Di et al. is a simple and rapid method to predict passive BBB permeation [33]. Compounds **6a-d**, **8a-b**, **9a-b**, **14b** and **15b** with sub-micromolar inhibitory activity for AChE were selected for test. After comparing experimental permeabilities of 9 commercial drugs with reported values (Table 2), a plot of experiment data versus the bibliographic values gave a good linear correlation: P_e (exp.) = 0.9075 P_e (bibl.) − 0.2016 (R_2 = 0.9654) (Fig. 4). From this equation and taking into account the limits established by Di et al. for BBB permeation, we classified compounds as follows:

(a) 'CNS+' (high BBB permeation predicted): P_e (10^{-6} cm/s) > 3.43
(b) 'CNS-' (low BBB permeation predicted): P_e (10^{-6} cm/s) < 1.61
(c) 'CNS ± ' (low BBB permeation predicted): 1.61 < P_e (10^{-6} cm/s) < 3.43

According to the measured permeabilities shown in Table 2, all compounds exhibited the P_e values higher than 3.43, which indicated that these selected compounds could cross the BBB and exert the biological effects in the CNS.

2.6. Inhibition studies of self-induced Aβ aggregation

As all selected compounds could cross the BBB, we next tested their ability to inhibit amyloid-β (Aβ) aggregation. The abilities of compounds to inhibit self-induced $Aβ_{1-42}$ aggregation was evaluated using a thioflavin T (ThT) fluorometric assay [34,35]. Curcumin, a well-known natural inhibitor for $Aβ_{1-42}$ self-aggregation, was taken as reference compound. From the results summarized in Table 3, it can be seen that these compounds exhibit moderate to good potencies (15.04–38.56% at 25 μM) compared with curcumin (38.59% at 25 μM). Among these compounds, compounds **6b**, **6c** and **9a** (38.56%, 38.25%, and 38.38% at 25 μM, respectively) exhibited the best inhibitory activity for $Aβ_{1-42}$ aggregation, which were comparable to that of curcumin.

2.7. Inhibition studies of AChE-induced Aβ aggregation

Accumulating evidences indicate that the PAS of AChE can bind to Aβ and promote the formation of amyloid fibrils. Therefore, inhibition of AChE, especially for the inhibition of PAS of AChE, may reduce Aβ aggregation. Since the studies above have proved that our present compounds were able to bind both CAS and PAS of AChE, compounds **6a-d**, **8a-b**, **9a-b**, **14b** and **15b** were also selected to detect their inhibitory activities against AChE-induced $Aβ_{1-42}$ aggregation. The inhibitory activities were also determined by the ThT method, and a dual binding site inhibitor of AChE, donepezil, was chosen as reference compound [36,37]. As shown in the Table 3, most compounds exhibit effectively inhibitory activity for AChE-induced $Aβ_{1-42}$ aggregation

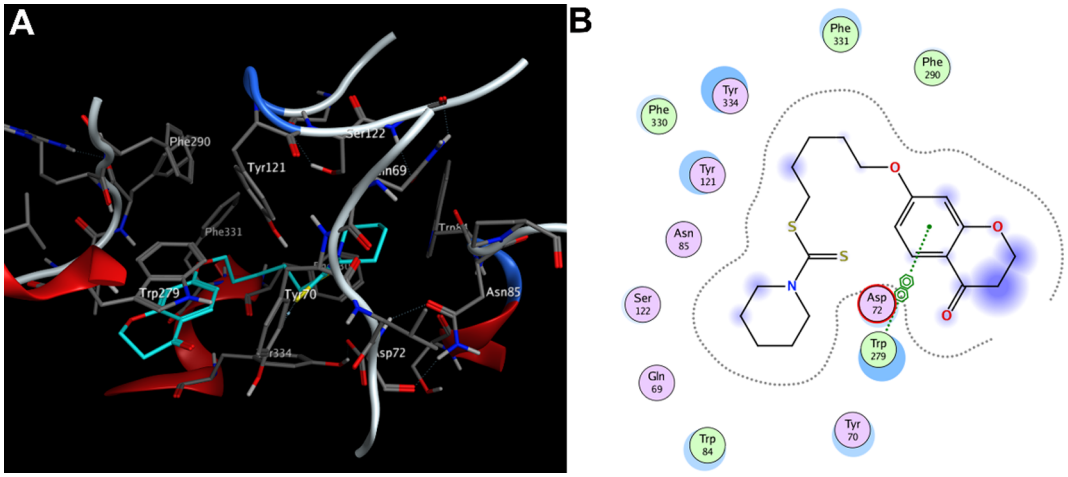

Fig. 3. (a) 3D docking model of compound **6c** with *Tc*AChE. Atom colours: cyan-carbon atoms of compound **6c**, grey-carbon atoms of residues of *Tc*AChE, dark blue-nitrogen atoms, red-oxygen atoms, yellow-sulfur atom. (b) 2D schematic diagram of docking model of compound **6c** with *Tc*AChE. The figure was prepared using the ligand interactions application in MOE. The green dashed line represents the interaction between the protein and the ligand.

Table 2
Permeability P_e ($\times 10^{-6}$) in the PAMPA-BBB assay for 9 commercial drugs in the experiment validation.

Commercial drugs	Bibliography[a]	Experiment[b]	Compd.	P_e ($\times 10^{-6}$ cm/s)
Testosterone	17.0	14.8 ± 0.85	**6a**	7.55 ± 0.64
Estradiol	12.0	9.83 ± 0.73	**6b**	7.67 ± 0.82
Progesterone	9.3	9.52 ± 0.62	**6c**	7.83 ± 0.51
Chlorpromazine	6.5	7.55 ± 0.54	**6d**	7.62 ± 0.98
Corticosterone	5.1	3.56 ± 0.62	**8a**	8.14 ± 0.73
Hydrocortisone	1.9	0.63 ± 0.06	**8b**	7.96 ± 0.61
Caffeine	1.3	1.12 ± 0.24	**9a**	7.24 ± 0.39
Atenolol	1.02	0.21 ± 0.02	**9b**	8.02 ± 0.76
Theophylline	0.1	0.17 ± 0.01	**14b**	7.26 ± 0.36
–	–	–	**15b**	7.91 ± 0.45

[a] Taken for Ref. [33].
[b] Experimental data are expressed as mean ± SD from three independent experiments, using PBS: EtOH (70:30) as solvent.

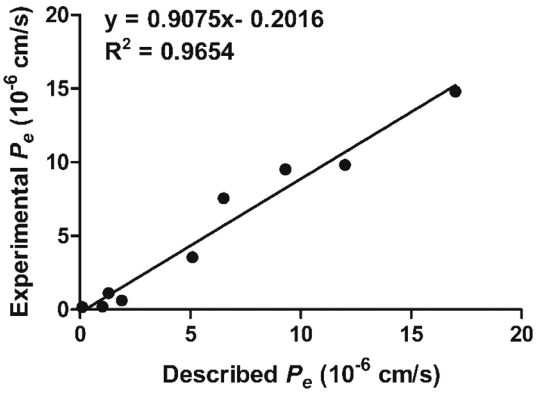

Fig. 4. Lineal correlation between experimental and reported permeability of commercial drugs using the PAMPA-BBB assay. P_e (exp.) = 0.9075 P_e (bibl.) − 0.2016 (R_2 = 0.9654).

with inhibition rate ranging from 14.75 to 33.02% at 100 μM in comparison to donepezil (27.13%). Compounds **6b** and **6c** possessing higher inhibitory activity for eeAChE also showed stronger activity to inhibit the aggregation. Compound **6c** displayed the strongest inhibitory activity in this series with inhibition rate of 33.02%, which was more potent than that of donepezil. After completing all above biological evaluations, compound **6c** with good BBB permeability and potent inhibitory activity to eeAChE and self- and AChE-induced Aβ aggregation was selected as a promising compound for further study.

Table 3
Inhibition of AChE-induced and self-induced $A\beta_{1\text{-}42}$ aggregation by selected compounds.

Compd.	Inhibition of $A\beta_{1\text{-}42}$ aggregation (%)	
	Self-induced[a]	AChE-induced[b]
6a	18.43 ± 2.87	19.67 ± 1.02
6b	38.56 ± 5.62	30.46 ± 2.19
6c	38.25 ± 3.84	33.02 ± 3.55
6d	20.11 ± 2.02	14.75 ± 2.53
8a	36.24 ± 1.96	27.17 ± 2.16
8b	35.76 ± 5.37	29.32 ± 3.10
9a	38.38 ± 2.18	23.84 ± 2.14
9b	37.24 ± 3.44	25.13 ± 3.27
14b	15.04 ± 1.10	15.25 ± 1.03
15b	19.11 ± 0.93	18.22 ± 2.04
Donepezil	–	27.13 ± 1.93
Curcumin	38.59 ± 2.17	–

[a] Inhibition of self-induced $A\beta_{1\text{-}42}$ aggregation (means ± SD of three experiments). The thioflavin-T fluorescence method was used, and the measurements were carried out in the presence of 25 μM inhibitor.
[b] Inhibition of AChE-induced $A\beta_{1\text{-}42}$ aggregation (means ± SD of three experiments). The thioflavin-T fluorescence method was used, and the concentration of the tested inhibitor was 100 μM.

2.8. Cytotoxicity of human neuroblastoma SH-SY5Y cells

To check the potential toxicity of compound **6c** to nerve cells, its cytotoxicity was evaluated using the human neuroblastoma SH-SY5Y cell line, and donepezil was taken as reference compound. After treating the cells with **6c** or donepezil at different concentrations (12.5, 25, 50 and 100 μM) for 24 h, the cell viability was determined by 3-(4,5-dimethylthiazol-2-yl)-2,5-diphenyltetrazolium (MTT) assay [38]. As shown in Fig. 5, similar to donepezil, compound **6c** did not cause any toxicity to SH-SY5Y cells even at the highest concentration, which indicated that it might be a safe multifunctional inhibitor for AD treatment.

2.9. Acute oral toxicity studies

To further investigate the safety property of compound **6c**, an acute toxicity evaluation was performed in KM mice (18–25 g, n = 10 per group, half male and half female) [24,25,39]. After delivering

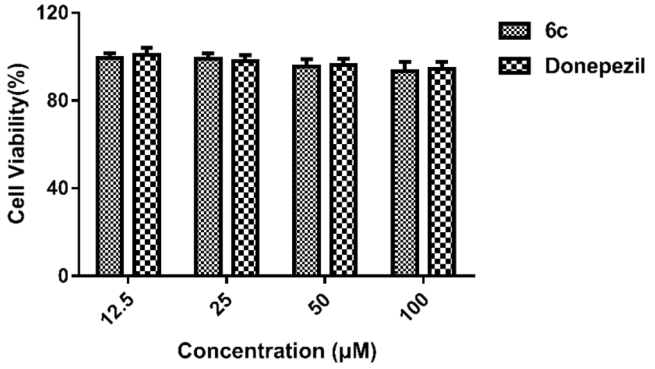

Fig. 5. Cytotoxicity of compound **6c** and donepezil on human neuroblastoma cells SH-SY5Y. SH-SY5Y cells were incubated with different concentrations of compound **6c** or donepezil (12.5–100 μM) for 24 h. The results are shown as the percentage of viable cells after treatment with compound **6c** or donepezil *vs* untreated control cells. Date are expressed as mean ± SD from three independent experiments.

compound **6c** to mice with various dosages (625, 1250 and 2500 mg/kg) by oral administration, no abnormal behavior and acute toxicity, such as death, marked weight loss, and drastically altered consumption of water or food, were detected during the experimental period. In addition, the possible toxic damage on organs of the mice was also examined after sacrificing these animals on the 14th day. The results indicated that no toxic effect was observed on heart, liver or kidneys, which demonstrated that compound **6c** was well tolerated at a dose up to 2500 mg/kg.

2.10. In vivo step-down passive avoidance assay

Given the excellent results obtained from above experiments, we next performed a step-down passive avoidance test to determine whether compound **6c** could improve memory impairment in vivo. The scopolamine was used as an inducer to establish the cognitive deficit mouse model and donepezil was selected as the positive control [40,41]. It can be seen from the Fig. 6 that model group show significantly reduced the latency and increased the number of errors in comparison to the control group ($^{###}p < 0.001$). When mice were treated with compound **6c**, the step-down latency and number of errors were reversed in a dose-dependent manner. The high dose group (83.2 mg/kg) showed the longest latency (221.0) and the least number of errors (1) among these groups, which were better than those of donepezil group (5 mg/kg, 200.9 s, 1.1). Meanwhile, the medium dose group (41.6 mg/kg) also exhibited the effects comparable (201.3 s; 1.2) to those of donepezil. Finally, compared with model group, although the low dose group (20.8 mg/kg) did not showed a significant difference, the latency and number of errors were largely improved (155.2 s *vs* 123.0 s, 1.9 *vs* 2.7). Altogether, the above results indicated that compound **6c** could attenuate the cognitive deficit through increasing the cholinergic activity in brain by inhibition of AChE.

3. Conclusion

A series of new hybrid molecules by connecting chromanone with dithiocarbamate moieties through flexible linkers have been designed and synthesized as multifunctional AChE inhibitors for the treatment of AD. Biological assays indicated that most of these compounds presented potent inhibitory activity and high selectivity for eeAChE. Of these compounds, compound **6c** stood out as the most potent inhibitor to eeAChE, showing the IC_{50} values of 0.10 μM, which was 4.5-fold more potent than that of tacrine. Kinetic analysis revealed that compound **6c** was a mix-type inhibitor of AChE. Further docking studies confirmed that **6c** was a dual binding site inhibitor, which could interact simultaneously with the PAS and CAS of AChE. Besides, compound **6c** also displayed the best activity to inhibit AChE-induced Aβ aggregation and potent activity to inhibit self-induced Aβ aggregation. Meanwhile, it could cross the BBB and showed good safety profiles in both cell and animal tests. At last, the step-down passive avoidance assay indicated that compound **6c** could significantly ameliorate the cognitive dysfunction induced by scopolamine in mice (83.2 and 41.6 mg/kg, p.o.). Overall, the present results suggest that compound **6c** is a potential disease-modifying agent for treating AD, and the dithiocarbamate moiety could be considered as a valid scaffold for design of multifunctional AChE inhibitors.

4. Experimental section

4.1. Chemistry

All chemicals and solvents were obtained from commercial sources and were used without purification. Reactions were monitored using thin-layer chromatography (TLC) on glass-packed precoated silica gel plates and visualized with a UV lamp. Column chromatography was performed using silica gel (200–300 mesh) purchased from Qingdao Haiyang Chemical Co. Ltd. Melting points were measured on an XT-4 micro melting point apparatus and were uncorrected. ^{1}H NMR spectra (500 MHz) and ^{13}C NMR spectra (126 MHz) were recorded on a Bruker ACF-600 spectrometer at room temperature using $CDCl_3$ or DMSO-d_6 as

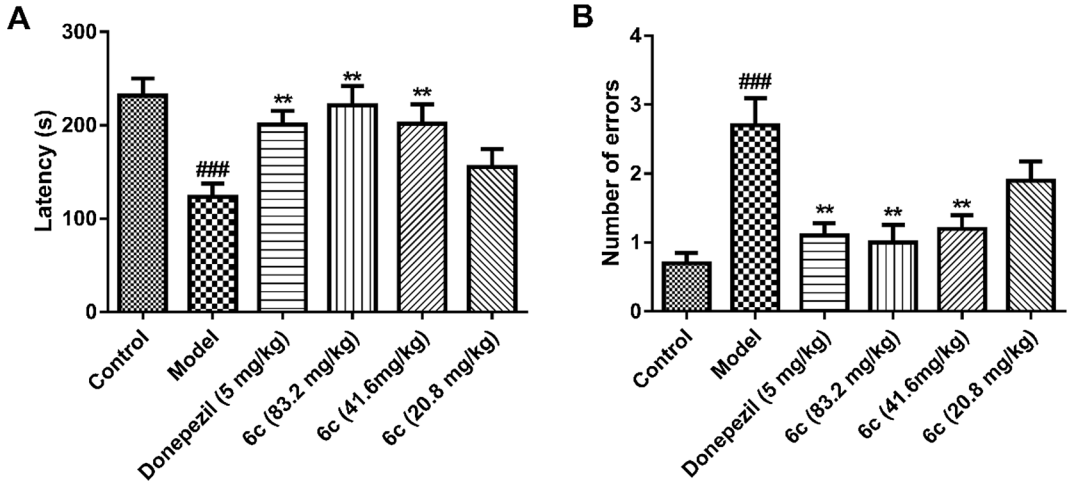

Fig. 6. Effects of compound **6c** on the (a) latency (s) and (b) number of errors in the step-down test by the scopolamine-induced cognitive impairment. The data shown are mean ± SD (n = 8). $^{###}P < 0.001$ *vs*. control group, $^{*}P < 0.05$, $^{**}P < 0.01$ *vs*. model group.

the solvent. Chemical shifts (δ) are reported in parts per million (ppm) using the tetramethylsilane (TMS) as internal standard. The coupling constants J are presented in hertz (Hz). The ESI-MS spectra were obtained on LCQ Fleet LC-MS System (Thermo Fisher Scientific, USA). The high-resolution mass spectra (HRMS) were recorded with a TripleTOF 5600 System (AB SCIEX). The purity (> 95%) of all final compounds was determined by HPLC, conducted on a Shimadzu LC-20AT series system, TC-C18 column (4.6 mm × 150 mm, 5 μm), eluted with MeOH/H_2O = 85/15, at a flow rate of 1.0 mL/min.

4.2. 3-Chloro-1-(2,4-dihydroxyphenyl)propan-1-one (3)

To a stirred mixture of resorcinol (5.0 g, 45.4 mmol) and 3-chloropropionic acid (4.9 g, 45.4 mmol), trifluoromethanesulfonic acid (13.6 g, 90.8 mmol) was added. After heating the mixture at 80 °C for 30 min, the reaction mixture was allowed to cool to room temperature and poured into ice cooled water (100 mL). Then, the mixture was extracted with Cl_2CH_2. The combined organic phase was washed with brine, dried over anhydrous Na_2SO_4 and concentrated under vacuum to afford crude product as orange oil. Without further purification, the crude product was directly used in next step.

4.3. 7-Hydroxychroman-4-one (4)

To a cooled 2 N aqueous NaOH was added crude compound **3**. The resulting solution was stirred at room temperature for 2 h and then cooled to 5 °C. The solution was acidified with 6 M H_2SO_4 to pH = 2. The mixture was extracted with ethyl acetate. The combined organic phase was washed with brine, dried over anhydrous Na_2SO_4 and concentrated under vacuum to afford crude product as brown solid. Yield 62%; brown solid; ^{1}H NMR (500 MHz, $CDCl_3$) δ 7.83 (d, J = 8.7 Hz, 1H, Ar−H), 6.54 (dd, J = 8.7, 2.3 Hz, 1H, Ar−H), 6.41 (d, J = 2.3 Hz, 1H, Ar−H), 4.57–4.46 (m, 2H, −OCH_2−), 2.84–2.72 (m, 2H, −COCH_2−); ^{13}C NMR (126 MHz, $CDCl_3$) δ 191.4, 164.2, 163.2, 129.7, 115.4, 110.7, 103.3, 67.4, 37.5.

4.4. General procedure for synthesis of compounds 5a-d

Compound **4** (5.0 mmol) and anhydrous K_2CO_3 (1.4 g, 10 mmol) were suspended in acetone (15 mL). Then, suitable α, ω-dibromoalkanes (50 mmol) was added, and the mixture was stirred under reflux for 4 h. When the reaction was completed, the reaction mixture was filtered, and the filtrate was concentrated under reduced pressure. The obtained residue was purified by silica gel chromatography with PE/EA (16:1) as eluent to give compounds **5a-d**.

4.4.1. 7-(3-bromopropoxy)chroman-4-one (5a)

Yield 75%; white solid; m.p. 86–88 °C; ^{1}H NMR (500 MHz, $CDCl_3$) δ 7.81 (d, J = 8.8 Hz, 1H, Ar−H), 6.54 (dd, J = 8.8, 2.3 Hz, 1H, Ar−H), 6.37 (d, J = 2.3 Hz, 1H, Ar−H), 4.59–4.39 (m, 2H, −OCH_2−), 4.09 (t, J = 6.4 Hz, 2H, −OCH_2−), 3.60 (t, J = 6.0 Hz, 2H, −CH_2Br), 2.86–2.67 (m, 2H, −COCH_2−), 2.35–2.29 (m, 2H, −CH_2−). ^{13}C NMR (126 MHz, $CDCl_3$) δ 190.6, 165.3, 163.8, 129.0, 115.3, 110.3, 101.3, 67.4, 67.1, 37.5, 34.9, 30.1.

4.4.2. 7-(4-bromobutoxy)chroman-4-one (5b)

Yield 69%; white solid; m.p. 58–60 °C; ^{1}H NMR (500 MHz, $CDCl_3$) δ 7.80 (d, J = 8.8 Hz, 1H, Ar−H), 6.54 (dd, J = 8.8, 2.3 Hz, 1H, Ar−H), 6.37 (d, J = 2.3 Hz, 1H, Ar−H), 4.49 (t, J = 6.4 Hz, 2H, −OCH_2−), 4.00 (t, J = 6.0 Hz, 2H, −OCH_2−), 3.46 (t, J = 6.5 Hz, 2H, −CH_2Br), 2.87–2.64 (m, 2H, −COCH_2−), 2.07–2.01 (m, 2H, −CH_2−), 1.96–1.91 (m, 2H, −CH_2−).^{13}C NMR (126 MHz, $CDCl_3$) δ 190.6, 165.3, 163.8, 129.0, 115.4, 110.2, 101.3, 67.4, 67.3, 37.5, 33.3, 29.4, 27.7.

4.4.3. 7-((5-bromopentyl)oxy)chroman-4-one (5c)

Yield 62%; white solid; m.p. 56–58 °C; ^{1}H NMR (500 MHz, $CDCl_3$) δ 7.81 (d, J = 8.8 Hz, 1H, Ar−H), 6.55 (dd, J = 8.8, 2.3 Hz, 1H, Ar−H), 6.37 (d, J = 2.3 Hz, 1H, Ar−H), 4.60–4.38 (m, 2H, −OCH_2−), 3.98 (t, J = 6.3 Hz, 2H, −OCH_2−), 3.42 (t, J = 6.7 Hz, 2H, −CH_2Br), 2.87–2.58 (m, 2H, −COCH_2−), 1.95–1.89 (m, 2H, −CH_2−), 1.84–1.78 (m, 2H, −CH_2−), 1.60 (p, J = 7.6 Hz, 2H, −CH_2−).^{13}C NMR (126 MHz, $CDCl_3$) δ 190.6, 165.4, 163.9, 128.9, 115.3, 110.3, 101.3, 68.1, 67.4, 37.5, 33.6, 32.4, 28.2, 24.8.

4.4.4. 7-((6-bromohexyl)oxy)chroman-4-one (5d)

Yield 67%; white solid; m.p. 54–56 °C; ^{1}H NMR (500 MHz, $CDCl_3$) δ 7.81 (d, J = 8.8 Hz, 1H, Ar−H), 6.55 (dd, J = 8.8, 1.7 Hz, 1H, Ar−H), 6.37 (d, J = 1.9 Hz, 1H, Ar−H), 4.50 (t, J = 6.4 Hz, 2H, −OCH_2−), 3.97 (t, J = 6.8 Hz, 2H, −OCH_2−), 3.41 (t, J = 6.7 Hz, 2H, −CH_2Br), 2.74 (t, J = 5.9 Hz, 2H, −COCH_2−), 1.88 (p, J = 6.5 Hz, 2H, −CH_2−), 1.80 (p, J = 6.4 Hz, 2H, −CH_2−), 1.55–1.42 (m, 4H, −CH_2−).^{13}C NMR (126 MHz, $CDCl_3$) δ 190.6, 165.5, 163.9, 129.0, 115.3, 110.3, 101.3, 68.3, 67.5, 37.5, 33.9, 32.7, 28.9, 28.0, 25.3.

4.5. General procedure for synthesis of compounds 6–18

To a solution of the secondary amine (1.2 mmol) and TEA (131 mg, 1.3 mmol) in DMF (2 mL) was added CS_2 (99 mg, 1.3 mmol) dropwise. After stirring the mixture for 5 min, appropriate chromanone derivatives **5a-d** (1.2 mmol) dissolved in DMF (3 mL) was added, and the mixture was stirred at room temperature for 12 h. After completion, the mixture was diluted with 20 mL of water and extracted with ethyl acetate. The combined organic phase was washed with water (15 mL × 3), dried over anhydrous Na_2SO_4, concentrated under vacuum, and purified by silica gel chromatography with PE/EA (10:1) as eluent to give the desire compounds **6–18**.

4.5.1. 3-((4-oxochroman-7-yl)oxy)propyl piperidine-1-carbodithioate (6a)

Yield 85%; white solid; m. p. 127–129 °C; ^{1}H NMR (500 MHz, $CDCl_3$) δ 7.76 (d, J = 8.8 Hz, 1H, Ar−H), 6.51 (dd, J = 8.8, 2.4 Hz, 1H, Ar−H), 6.34 (d, J = 2.4 Hz, 1H, Ar−H), 4.45 (t, J = 6.4 Hz, 2H, −OCH_2−), 4.23 (br s, 2H, −NCH_2−), 4.03 (t, J = 6.1 Hz, 2H, −OCH_2−), 3.81 (d, J = 8.0 Hz, 2H, −NCH_2−), 3.41 (t, J = 7.0 Hz, 2H, -SCH_2-), 2.67 (t, J = 6.4 Hz, 2H, −COCH_2−), 2.18–2.12 (m, 2H, −CH_2−), 1.63 (br s, 6H, −(CH_2)$_3$−). ^{13}C NMR (126 MHz, $CDCl_3$) δ 194.1, 189.5, 164.2, 162.8, 127.9, 114.3, 109.3, 100.3, 66.4, 65.8, 51.8, 50.3, 36.4, 32.3, 28.7, 23.3; ESI-MS m/z: 365.96 $[M + H]^+$; HRMS: calcd for $C_{18}H_{24}NO_3S_2$ $[M + H]^+$ 366.1192, found 366.1189. HPLC purity, 98.39%.

4.5.2. 4-((4-oxochroman-7-yl)oxy)butyl piperidine-1-carbodithioate (6b)

Yield 82%; White solid; m. p. 95–97 °C; ^{1}H NMR (500 MHz, $CDCl_3$) δ 7.83 (d, J = 8.8 Hz, 1H, Ar−H), 6.57 (dd, J = 8.8, 2.4 Hz, 1H, Ar−H), 6.39 (d, J = 2.3 Hz, 1H, Ar−H), 4.51 (t, J = 6.5 Hz, 2H, −OCH_2−), 4.31–4.29 (m, 2H, −NCH_2−), 4.02 (t, J = 6.5 Hz, 2H, −OCH_2−), 3.89 (br s, 2H, −NCH_2−), 3.38 (t, J = 6.5 Hz, 2H, −SCH_2−), 2.75 (t, J = 6.5 Hz, 2H, −COCH_2−), 1.94–1.87 (m, 4H, −(CH_2)$_2$−), 1.73–1.68 (m, 6H, −(CH_2)$_3$−).^{13}C NMR (126 MHz, $CDCl_3$) δ 195.7, 190.7, 165.5, 163.9, 129.0, 115.3, 110.4, 101.3, 67.9, 67.5, 53.1, 51.4, 37.6, 36.7, 28.4, 25.6, 24.5; ESI-MS m/z: 380.03 $[M + H]^+$; HRMS: calcd for $C_{19}H_{26}NO_3S_2$ $[M + H]^+$ 380.1348, found 380.1346. HPLC purity, 97.32%.

4.5.3. 5-((4-oxochroman-7-yl)oxy)pentyl piperidine-1-carbodithioate (6c)

Yield 87%; white solid; m. p. 70–71 °C; ^{1}H NMR (500 MHz, $CDCl_3$) δ 7.82 (d, J = 8.8 Hz, 1H, Ar−H), 6.57 (dd, J = 8.8, 2.4 Hz, 1H, Ar−H), 6.38 (d, J = 2.4 Hz, 1H, Ar−H), 4.50 (t, J = 6.4 Hz, 2H, −OCH_2−), 4.25 (br s, 2H, −NCH_2−), 3.98 (t, J = 6.4 Hz, 2H, −OCH_2−), 3.91 (br s, 2H, −NCH_2−), 3.32 (t, J = 6.5 Hz, 2H, −SCH_2−), 2.74 (t, J = 6.0 Hz, 2H, −COCH_2−), 1.85–1.56 (m, 12H, −(CH_2)$_6$−).^{13}C NMR (126 MHz, $CDCl_3$) δ 195.8, 190.6, 165.5, 163.8, 128.9, 115.2, 110.3, 101.2, 68.2, 67.4, 52.9, 51.4, 37.5, 36.9, 28.6, 25.4, 24.4; ESI-MS m/z: 394.07

$[M + H]^+$; HRMS: calcd for $C_{20}H_{28}NO_3S_2$ $[M + H]^+$ 394.1505, found 394.1506. HPLC purity, 98.55%.

*4.5.4. 3 6-((4-oxochroman-7-yl)oxy)hexyl piperidine-1-carbodithioate (**6d**)*

Yield 87%; yellow oil; ^{1}H NMR (500 MHz, $CDCl_3$) δ 7.76 (d, J = 8.8 Hz, 1H, Ar−H), 6.50 (dd, J = 8.8, 2.4 Hz, 1H, Ar−H), 6.32 (d, J = 2.4 Hz, 1H, Ar−H), 4.44 (t, J = 6.4 Hz, 2H, −OCH_2−), 4.21 (d, J = 6.6 Hz, 2H, −NCH_2−), 3.91 (t, J = 6.5 Hz, 2H, −OCH_2−), 3.84 (br s, 2H, −NCH_2−), 3.24 (t, J = 7.5 Hz, 2H, -SCH_2-), 2.68 (t, J = 6.5 Hz, 2H, −COCH_2−), 1.80–1.60 (m, 10*H*, −(CH_2)$_5$−), 1.44–1.41 (m, 4H, −(CH_2)$_2$−).^{13}C NMR (126 MHz, $CDCl_3$) δ 194.9, 189.6, 164.5, 162.8, 127.8, 114.1, 109.3, 100.2, 67.3, 66.4, 51.8, 50.3, 36.4, 36.0, 27.8, 27.7, 24.6, 23.3; ESI-MS *m/z*: 408.01$[M + H]^+$; HRMS: calcd for $C_{21}H_{30}NO_3S_2$ $[M + H]^+$ 408.1661, found408.1672. HPLC purity, 98.83%.

*4.5.5. 4-((4-oxochroman-7-yl)oxy)butyl 4-methylpiperidine-1-carbodithioate (**7a**)*

Yield 87%; white solid; m. p. 60–61 °C; ^{1}H NMR (500 MHz, DMSO-d_6) δ 7.68 (d, J = 8.8 Hz, 1H, Ar−H), 6.63 (dd, J = 8.8, 2.3 Hz, 1H, Ar−H), 6.53 (d, J = 2.3 Hz, 1H, Ar−H), 4.50 (t, J = 6.4 Hz, 2H, −OCH_2−), 4.06 (t, J = 6.0 Hz, 2H, −OCH_2−), 3.29 (br s, 4H, −NCH_2−), 2.71 (t, J = 6.4 Hz, 2H, −COCH_2−), 1.83–1.72 (m, 8H, −(CH_2)$_4$−), 1.24 (s, 1H, −CH−), 1.19–1.04 (m, 2H, −CH_2−), 0.92 (s, 3H, −CH_3). ^{13}C NMR (126 MHz, DMSO-d_6) δ 194.5, 190.6, 165.3, 164.0, 128.7, 115.4, 110.6, 101.9, 68.2, 67.7, 52.1, 50.5, 37.5, 36.4, 30.6, 28.2, 25.7, 21.7; ESI-MS *m/z*: 394.05 $[M + H]^+$; HRMS: calcd for $C_{20}H_{28}NO_3S_2$ $[M + H]^+$ 394.1505, found 394.1516. HPLC purity, 96.43%.

*4.5.6. 5-((4-oxochroman-7-yl)oxy)pentyl 4-methylpiperidine-1-carbodithioate (**7b**)*

Yield 87%; white solid; m. p. 60–62 °C; ^{1}H NMR (500 MHz, $CDCl_3$) δ 7.81 (d, J = 8.8 Hz, 1H, Ar−H), 6.55 (dd, J = 8.8, 2.3 Hz, 1H, Ar−H), 6.37 (d, J = 2.3 Hz, 1H, Ar−H), 4.49 (t, J = 6.4 Hz, 2H, −OCH_2−), 3.97 (t, J = 6.4 Hz, 2H, −OCH_2−), 3.30 (br s, 2H, −NCH_2−), 3.13–3.05 (m, 2H, −NCH_2−), 2.73 (t, J = 6.4 Hz, 2H, −COCH_2−), 1.85–1.68 (m, 8H, −(CH_2)$_4$−), 1.60–1.55 (m, 2H, −CH_2−), 1.26 (br s, 3H, −CHCH_2−), 0.96 (s, 3H, −CH_3). ^{13}C NMR (126 MHz, $CDCl_3$) δ 195.9, 190.6, 165.5, 163.8, 128.9, 115.2, 110.3, 101.2, 68.2, 67.4, 52.1, 50.4, 37.5, 37.0, 31.0, 28.6, 28.5, 25.4, 21.3. ESI-MS *m/z*: 408.08 $[M + H]^+$; HRMS: calcd for $C_{21}H_{30}NO_3S_2$ $[M + H]^+$408.1661, found 408.1660. HPLC purity, 96.16%.

*4.5.7. 4-((4-oxochroman-7-yl)oxy)butyl 2-methylpiperidine-1-carbodithioate (**8a**)*

Yield 87%; white solid; m. p. 46–47 °C; ^{1}H NMR (500 MHz, $CDCl_3$) δ 7.85 (d, J = 8.8 Hz, 1H, Ar−H), 6.59 (dd, J = 8.8, 2.4 Hz, 1H, Ar−H), 6.41 (d, J = 2.4 Hz, 1H, Ar−H), 4.53 (t, J = 6.0 Hz, 2H, −OCH_2−), 4.05 (t, J = 6.0 Hz, 2H, −OCH_2−), 3.41 (t, J = 7.0 Hz, 2H, −NCH_2−), 3.15 (br s, 1H, −NCH−), 2.77 (t, J = 7.2 Hz, 2H, −COCH_2−), 1.98–1.88 (m, 4H, −(CH_2)$_2$−), 1.80–1.63 (m, 8H, −(CH_2)$_4$−), 1.29 (d, J = 7.0 Hz, 3H, −CH_3). ^{13}C NMR (126 MHz, $CDCl_3$) δ 195.9, 190.6, 165.4, 163.8, 128.9, 115.2, 110.3, 101.2, 67.8, 67.4, 54.0, 37.4, 36.4, 28.3, 25.4, 18.7. ESI-MS *m/z*: 394.05 $[M + H]^+$; HRMS: calcd for $C_{20}H_{27}NO_3S_2Na$ $[M + Na]^+$ 416.1325, found 416.1339. HPLC purity, 95.99%.

*4.5.8. 5-((4-oxochroman-7-yl)oxy)pentyl 2-methylpiperidine-1-carbodithioate (**8b**)*

Yield 87%; white solid; m. p. 46–48 °C; ^{1}H NMR (500 MHz, $CDCl_3$) δ 7.76 (d, J = 8.8 Hz, 1H, Ar−H), 6.50 (dd, J = 8.8, 2.4 Hz, 1H, Ar−H), 6.32 (d, J = 2.3 Hz, 1H, Ar−H), 4.44 (t, J = 6.5 Hz, 2H, −OCH_2−), 3.93 (t, J = 6.4 Hz, 2H, −OCH_2−), 3.25 (t, J = 7.5 Hz, 2H, −NCH_2−), 3.06 (br s, 1H, −NCH−), 2.69 (t, J = 6.5 Hz, 2H, −COCH_2−), 1.80–1.65 (m, 8H, −(CH_2)$_4$−), 1.62–1.49 (m, 6H, −(CH_2)$_3$−), 1.21 (d, J = 7.0 Hz, 3H, −CH_3). ^{13}C NMR (126 MHz, $CDCl_3$) δ 195.1, 189.5, 164.5, 162.8, 127.8, 114.1, 109.2, 100.2, 67.1, 66.3, 52.7, 36.4, 35.7, 27.5, 27.4, 24.4, 17.6; ESI-MS *m/z*: 408.05 $[M + H]^+$; HRMS: calcd for $C_{21}H_{30}NO_3S_2$ $[M + H]^+$408.1662, found 408.1681. HPLC purity, 98.53%.

*4.5.9. 4-((4-oxochroman-7-yl)oxy)butyl 2,6-dimethylpiperidine-1-carbodithioate (**9a**)*

Yield 87%; white solid; m. p. 81–82 °C; ^{1}H NMR (500 MHz, $CDCl_3$) δ 7.85 (d, J = 8.8 Hz, 1H, Ar−H), 6.59 (dd, J = 8.9, 2.3 Hz, 1H, Ar−H), 6.41 (d, J = 2.3 Hz, 1H, Ar−H), 4.53 (t, J = 6.4 Hz, 2H, −OCH_2−), 4.05 (t, J = 5.9 Hz, 2H, −OCH_2−), 3.48–3.32 (m, 2H, −N(CH)$_2$−), 2.77 (t, J = 6.4 Hz, 2H, −COCH_2−), 2.00–1.52 (m, 12H, −(CH_2)$_6$−), 1.37 (d, J = 7.0 Hz, 3H, −CH_3), 1.33 (d, J = 7.1 Hz, 3H, −CH_3). ^{13}C NMR (126 MHz, $CDCl_3$) δ 196.6, 190.6, 165.4, 163.8, 128.9, 115.2, 110.3, 101.2, 67.8, 67.4, 53.6, 52.8, 37.4, 36.4, 30.4, 30.2, 28.3, 25.3, 19.8, 18.7, 14.0. ESI-MS *m/z*: 408.03 $[M + H]^+$; HRMS: calcd for $C_{21}H_{30}NO_3S_2$ $[M + H]^+$ 408.1662, found 408.1680. HPLC purity, 95.48%.

*4.5.10. 5-((4-oxochroman-7-yl)oxy)pentyl 2,6-dimethylpiperidine-1-carbodithioate (**9b**)*

Yield 87%; white solid; m. p. 57–59 °C; ^{1}H NMR (500 MHz, DMSO-d_6) δ 7.68 (d, J = 8.8 Hz, 1H, Ar−H), 6.63 (dd, J = 8.8, 2.4 Hz, 1H, Ar−H), 6.53 (d, J = 2.3 Hz, 1H, Ar−H), 4.50 (t, J = 6.4 Hz, 2H, −OCH_2−), 4.04 (t, J = 6.4 Hz, 2H, −OCH_2−), 3.33–3.20 (m, 2H, −N(CH)$_2$−), 2.70 (t, J = 6.4 Hz, 2H, −COCH_2−), 1.89–1.43 (m, 14H, −(CH_2)$_7$−), 1.28 (d, J = 7.0 Hz, 3H, −CH_3), 1.22 (d, J = 7.1 Hz, 3H, −CH_3).^{13}C NMR (126 MHz, DMSO-d_6) δ 196.0, 190.6, 165.4, 164.0, 128.7, 115.3, 110.5, 101.8, 68.5, 67.7, 53.7, 53.1, 37.5, 36.5, 30.4, 30.3, 28.6, 28.5, 25.5, 20.1, 18.9, 14.0. ESI-MS *m/z*: 422.02 $[M + H]^+$; HRMS: calcd for $C_{22}H_{32}NO_3S_2$ $[M + H]^+$422.1818, found 422.1840. HPLC purity, 98.52%.

*4.5.11. 4-((4-oxochroman-7-yl)oxy)butyl 4-hydroxypiperidine-1-carbodithioate (**10a**)*

Yield 87%; white solid; m. p.106–108 °C;^{1}H NMR (500 MHz, $CDCl_3$) δ 7.85 (d, J = 8.8 Hz, 1H, Ar−H), 6.59 (dd, J = 8.8, 2.3 Hz, 1H, Ar−H), 6.41 (d, J = 2.4 Hz, 1H, Ar−H), 4.53 (t, J = 6.0 Hz, 2H, −OCH_2−), 4.05 (t, J = 5.9 Hz, 2H, −OCH_2−), 3.81 (br s, 1H, −CHOH), 3.40 (t, J = 6.9 Hz, 2H, −NCH_2−), 2.77 (t, J = 6.5 Hz, 2H, −COCH_2−), 1.98–1.66 (m, 12H, −(CH_2)$_6$−).^{13}C NMR (126 MHz, $CDCl_3$) δ 196.2, 190.6, 165.4, 163.8, 128.9, 115.2, 110.3, 101.2, 67.8, 67.4, 66.2, 48.1, 46.6, 37.4, 36.8, 29.7, 28.2, 25.5. ESI-MS *m/z*: 396.06 $[M + H]^+$. HRMS: calcd for $C_{19}H_{26}NO_4S_2$ $[M + H]^+$ 396.1298, found 396.1304. HPLC purity, 95.69%.

*4.5.12. 5-((4-oxochroman-7-yl)oxy)pentyl 4-hydroxypiperidine-1-carbodithioate (**10b**)*

Yield 87%; white solid; m. p. 104–106 °C; ^{1}H NMR (500 MHz, $CDCl_3$) δ 7.84 (d, J = 8.8 Hz, 1H, Ar−H), 6.58 (dd, J = 8.8, 2.3 Hz, 1H, Ar−H), 6.39 (d, J = 2.2 Hz, 1H, Ar−H), 4.51 (t, J = 6.4 Hz, 2H, −OCH_2−), 4.00 (t, J = 6.4 Hz, 2H, −OCH_2−), 3.77 (br s, 1H, −CHOH), 3.33 (t, J = 7.4 Hz, 2H, −NCH_2−), 2.75 (t, J = 6.4 Hz, 2H, −COCH_2−), 1.96 (br s, 2H, −NCH_2−), 1.87–1.76 (m, 4H, −(CH_2)$_2$−), 1.70–1.57 (m, 8H, −(CH_2)$_4$−); ^{13}C NMR (126 MHz, $CDCl_3$) δ 196.6, 190.8, 165.6, 163.9, 129.0, 115.3, 110.4, 101.4, 68.3, 67.5, 66.4, 48.4, 46.8, 37.6, 37.3, 28.7, 28.6, 25.5. ESI-MS *m/z*: 410.02 $[M + H]^+$. HRMS: calcd for $C_{20}H_{28}NO_4S_2$ $[M + H]^+$ 410.1454, found 410.1482. HPLC purity, 95.69%.

*4.5.13. 4-((4-oxochroman-7-yl)oxy)butyl 4-phenylpiperidine-1-carbodithioate (**11a**)*

Yield 87%; yellow oil; ^{1}H NMR (500 MHz, DMSO-d_6) δ 7.69 (d, J = 8.8 Hz, 1H, Ar−H), 7.32–7.19 (m, 5H, Ar−H$_5$), 6.63 (dd, J = 8.8, 2.4 Hz, 1H, Ar−H), 6.54 (d, J = 2.3 Hz, 1H, Ar−H), 4.49 (t, J = 6.4 Hz, 2H, −OCH_2−), 4.07 (t, J = 5.9 Hz, 2H, −OCH_2−), 3.41 (br s, 2H, −NCH_2−), 3.22 (br s, 2H, −NCH_2−), 2.98–2.91 (m, 1H, Ar−CH−), 2.70

(t, J = 6.5 Hz, 2H, −COC$\underline{H}_2$−), 1.93–1.57 (m, 10*H*, -(C$\underline{H}_2$)$_5$-); ^{13}C NMR (126 MHz, DMSO-d_6) δ 194.8, 190.4, 165.2, 163.9, 145.3, 128.9, 128.6, 127.2, 126.8, 115.3, 110.4, 101.8, 68.1, 67.6, 52.1, 50.6, 41.8, 37.3, 36.4, 28.1, 25.6. ESI-MS *m/z*: 456.01 [M + H]$^+$; HRMS: calcd for $C_{25}H_{30}NO_3S_2$ [M + H]$^+$ 456.1662, found 456.1730. HPLC purity, 98.65%.

*4.5.14. 5-((4-oxochroman-7-yl)oxy)pentyl 4-phenylpiperidine-1-carbodithioate (**11b**)*

Yield 87%; yellow oil; ^{1}H NMR (500 MHz, $CDCl_3$) δ 7.77 (d, J = 8.8 Hz, 1H, Ar−$\underline{H}$), 7.26–7.23 (m, 2H, Ar−$\underline{H}_2$), 7.19–7.13 (m, 3H, Ar−$\underline{H}_3$), 6.51 (dd, J = 8.8, 2.4 Hz, 1H, Ar−$\underline{H}$), 6.33 (d, J = 2.3 Hz, 1H, Ar−$\underline{H}$), 4.44 (t, J = 6.0 Hz, 2H, −OC$\underline{H}_2$−), 3.93 (t, J = 6.4 Hz, 2H, −OC$\underline{H}_2$−), 3.29 (br s, 2H, −NC$\underline{H}_2$−), 3.15 (br s, 2H, −NC$\underline{H}_2$−), 2.83–2.79 (m, 1H, Ar−C$\underline{H}$−), 2.68 (t, J = 6.4 Hz, 2H, −COC$\underline{H}_2$−), 1.81–1.51 (m, 12H, −(C$\underline{H}_2$)$_6$−); ^{13}C NMR (126 MHz, $CDCl_3$) δ 195.4, 189.5, 164.5, 162.8, 143.4, 127.8, 127.6, 125.7, 125.7, 114.1, 109.3, 100.2, 67.1, 66.3, 51.2, 49.6, 41.7, 36.4, 36.0, 27.5, 27.5, 24.4. ESI-MS *m/z*: 470.02 [M + H]$^+$; HRMS: calcd for $C_{26}H_{32}NO_3S_2$ [M + H]$^+$470.1818, found470.1860. HPLC purity, 95.22%.

*4.5.15. 4-((4-oxochroman-7-yl)oxy)butyl pyrrolidine-1-carbodithioate (**12a**)*

Yield 87%; colorless oil; ^{1}H NMR (500 MHz, DMSO-d_6) δ 7.67 (d, J = 8.8 Hz, 1H, Ar−$\underline{H}$), 6.61 (dd, J = 8.8, 2.3 Hz, 1H, Ar−$\underline{H}$), 6.52 (d, J = 2.3 Hz, 1H, Ar−$\underline{H}$), 4.49 (t, J = 6.4 Hz, 2H, −OC$\underline{H}_2$−), 4.05 (t, J = 6.0 Hz, 2H, −OC$\underline{H}_2$−), 3.76 (t, J = 6.9 Hz, 2H, −NC$\underline{H}_2$−), 3.60 (t, J = 6.9 Hz, 2H, −NC$\underline{H}_2$−), 3.30 (t, J = 6.9 Hz, 2H, −SC$\underline{H}_2$−), 2.70 (t, J = 6.4 Hz, 2H, −COC$\underline{H}_2$−), 2.00 (p, J = 6.8 Hz, 2H, −C$\underline{H}_2$−), 1.90 (p, J = 6.8 Hz, 2H, −C$\underline{H}_2$−), 1.82 –1.74 (m, 4H, −(C$\underline{H}_2$)$_2$−); ^{13}C NMR (126 MHz, DMSO-d_6) δ 191.1, 190.1, 164.9, 163.5, 128.3, 114.9, 110.1, 101.4, 67.8, 67.2, 55.0, 50.6, 37.0, 35.2, 27.7, 25.7, 25.4, 23.9. ESI-MS *m/z*: 366.04 [M + H]$^+$; HRMS: calcd for $C_{18}H_{24}NO_3S_2$ [M + H]$^+$ 366.1192, found 366.1239. HPLC purity, 97.30%.

*4.5.16. 5-((4-oxochroman-7-yl)oxy)pentyl pyrrolidine-1-carbodithioate (**12b**)*

Yield 87%; white solid; m. p. 78–80 °C; ^{1}H NMR (500 MHz, DMSO-d_6) δ 7.67 (d, J = 8.8 Hz, 1H, Ar−$\underline{H}$), 6.62 (dd, J = 8.8, 2.3 Hz, 1H, Ar−$\underline{H}$), 6.52 (d, J = 2.3 Hz, 1H, Ar−$\underline{H}$), 4.49 (t, J = 6.4 Hz, 2H, −OC$\underline{H}_2$−), 4.02 (t, J = 6.4 Hz, 2H, −OC$\underline{H}_2$−), 3.75 (t, J = 6.9 Hz, 2H, −NC$\underline{H}_2$−), 3.59 (t, J = 6.9 Hz, 2H, −NC$\underline{H}_2$−), 3.24 (t, J = 7.3 Hz, 2H, −SC$\underline{H}_2$−), 2.70 (t, J = 6.4 Hz, 2H, −COC$\underline{H}_2$−), 2.00 (p, J = 6.8 Hz, 2H, −C$\underline{H}_2$−), 1.89 (p, J = 6.8 Hz, 2H, −C$\underline{H}_2$−), 1.76–1.64 (m, 4H, −(C$\underline{H}_2$)$_2$−), 1.51–1.45 (m, 2H, −C$\underline{H}_2$−). ^{13}C NMR (126 MHz, DMSO-d_6) δ 191.1, 190.1, 164.9, 163.5, 128.2, 114.9, 110.1, 101.4, 68.0, 67.2, 55.0, 50.6, 37.0, 35.4, 28.4, 28.1, 25.6, 24.8, 23.8. ESI-MS *m/z*: 380.01 [M + H]$^+$; HRMS: calcd for $C_{19}H_{26}NO_3S_2$ [M + H]$^+$ 380.1349, found 380.1353. HPLC purity, 98.22%.

*4.5.17. 4-((4-oxochroman-7-yl)oxy)butyl dimethylcarbamodithioate (**13a**)*

Yield 87%; white solid; m. p. 59–61 °C; ^{1}H NMR (500 MHz, DMSO-d_6) δ 7.67 (d, J = 8.8 Hz, 1H, Ar−$\underline{H}$), 6.61 (dd, J = 8.8, 2.4 Hz, 1H, Ar−$\underline{H}$), 6.52 (d, J = 2.3 Hz, 1H, Ar−$\underline{H}$), 4.50 (t, J = 6.4 Hz, 2H, −OC$\underline{H}_2$−), 4.05 (t, J = 6.1 Hz, 2H, −OC$\underline{H}_2$−), 3.45 (s, 3H, −NC$\underline{H}_3$), 3.39 (s, 3H, −NC$\underline{H}_3$), 3.28 (t, J = 7.0 Hz, 2H, −SC$\underline{H}_2$−), 2.70 (t, J = 6.4 Hz, 2H, −COC$\underline{H}_2$−), 1.83–1.73 (m, 4H, −(C$\underline{H}_2$)$_2$−).^{13}C NMR (126 MHz, DMSO-d_6) δ 195.8, 190.6, 165.3, 164.0, 128.7, 115.4, 110.6, 101.9, 68.2, 67.7, 45.5, 41.8, 37.5, 36.8, 28.2, 25.7. ESI-MS *m/z*: 340.02 [M + H]$^+$; HRMS: calcd for $C_{16}H_{22}NO_3S_2$ [M + H]$^+$ 340.1036, found 340.1050. HPLC purity, 95.48%.

*4.5.18. 5-((4-oxochroman-7-yl)oxy)pentyl dimethylcarbamodithioate (**13b**)*

Yield 87%; white clusters; m. p. 58–60 °C; ^{1}H NMR (500 MHz, $CDCl_3$) δ 7.81 (d, J = 8.8 Hz, 1H, Ar−$\underline{H}$), 6.56 (dd, J = 8.8, 2.3 Hz, 1H, Ar−$\underline{H}$), 6.37 (d, J = 2.2 Hz, 1H, Ar−$\underline{H}$), 4.50 (t, J = 6.4 Hz, 2H, −OC$\underline{H}_2$−), 3.98 (t, J = 6.4 Hz, 2H, −OC$\underline{H}_2$−), 3.54 (s, 3H, −NC$\underline{H}_3$), 3.35 (s, 3H, −NC$\underline{H}_3$), 3.30 (t, J = 7.4 Hz, 2H, −SC$\underline{H}_2$−), 2.73 (t, J = 6.4 Hz, 2H, −COC$\underline{H}_2$−), 1.85–1.79 (m, 2H, −C$\underline{H}_2$−), 1.76–1.73 (m, 2H, −C$\underline{H}_2$−), 1.61–1.55 (m, 2H, −C$\underline{H}_2$−). ^{13}C NMR (126 MHz, $CDCl_3$) δ 197.5, 190.7, 165.6, 163.9, 129.0, 115.3, 110.4, 101.3, 68.2, 67.5, 45.4, 41.6, 37.6, 37.5, 28.7, 28.6, 25.5. ESI-MS *m/z*: 354.09 [M + H]$^+$; HRMS: calcd for $C_{17}H_{24}NO_3S_2$ [M + H]$^+$ 354.1192, found 354.1196; HPLC purity, 98.01%.

*4.5.19. 4-((4-oxochroman-7-yl)oxy)butyl diethylcarbamodithioate (**14a**)*

Yield 87%; brown oil; ^{1}H NMR (500 MHz, DMSO-d_6) δ 7.67 (d, J = 8.8 Hz, 1H, Ar−$\underline{H}$), 6.62 (dd, J = 8.8, 2.4 Hz, 1H, Ar−$\underline{H}$), 6.52 (d, J = 2.3 Hz, 1H, Ar−$\underline{H}$), 4.50 (t, J = 6.4 Hz, 2H, −OC$\underline{H}_2$−), 4.05 (t, J = 6.0 Hz, 2H, −OC$\underline{H}_2$−), 3.96 (q, J = 7.0 Hz, 2H, −NC$\underline{H}_2$−), 3.74 (q, J = 7.0 Hz, 2H, −NC$\underline{H}_2$−), 3.28 (t, J = 7.0 Hz, 2H, −SC$\underline{H}_2$−), 2.70 (t, J = 6.4 Hz, 2H, −COC$\underline{H}_2$−), 1.82–1.74 (m, 4H, −(C$\underline{H}_2$)$_2$−), 1.21 (t, J = 7.1 Hz, 3H, −C$\underline{H}_3$), 1.17 (t, J = 7.0 Hz, 3H, −C$\underline{H}_3$).^{13}C NMR (126 MHz, DMSO-d_6) δ 194.4, 190.5, 165.2, 163.9, 128.6, 115.3, 110.5, 101.8, 68.1, 67.6, 49.4, 46.9, 37.4, 36.2, 28.1, 25.6, 12.8, 11.9. ESI-MS *m/z*: 368.06 [M + H]$^+$; HRMS: calcd for $C_{18}H_{26}NO_3S_2$ [M + H]$^+$ 368.1349, found 368.1362; HPLC purity, 97.00%.

*4.5.20. 5-((4-oxochroman-7-yl)oxy)pentyl diethylcarbamodithioate (**14b**)*

Yield 87%; yellow oil; ^{1}H NMR (500 MHz, DMSO-d_6) δ 7.67 (d, J = 8.8 Hz, 1H, Ar−$\underline{H}$), 6.62 (dd, J = 8.8, 2.4 Hz, 1H, Ar−$\underline{H}$), 6.52 (d, J = 2.3 Hz, 1H, Ar−$\underline{H}$), 4.49 (t, J = 6.4 Hz, 2H, −OC$\underline{H}_2$−), 4.03 (t, J = 6.4 Hz, 2H, −OC$\underline{H}_2$−), 3.95 (q, J = 7.0 Hz, 2H, −NC$\underline{H}_2$−), 3.73 (q, J = 7.1 Hz, 2H, −NC$\underline{H}_2$−), 3.23 (t, J = 6.4 Hz, 2H, −SC$\underline{H}_2$−), 2.70 (t, J = 6.4 Hz, 2H, −COC$\underline{H}_2$−), 1.76–1.64 (m, 4H, −(C$\underline{H}_2$)$_2$−), 1.52–1.46 (m, 2H, −C$\underline{H}_2$−), 1.20 (t, J = 6.5 Hz, 3H, −C$\underline{H}_3$), 1.16 (t, J = 7.1 Hz, 3H, −C$\underline{H}_3$); ^{13}C NMR (126 MHz, DMSO-d_6) δ 194.1, 190.1, 164.9, 163.5, 128.2, 114.9, 110.1, 101.4, 68.0, 67.2, 49.0, 46.5, 37.0, 36.1, 28.2, 28.1, 24.9, 12.5, 11.5. ESI-MS *m/z*: 382.02 [M + H]$^+$. HRMS: calcd for $C_{19}H_{27}NO_3S_2Na$ [M + Na]$^+$ 404.1325, found 404.1327; HPLC purity, 98.78%.

*4.5.21. 4-((4-oxochroman-7-yl)oxy)butyl diisopropylcarbamodithioate (**15a**)*

Yield 87%; yellow oil; ^{1}H NMR (500 MHz, $CDCl_3$) δ 7.85 (d, J = 8.8 Hz, 1H, Ar−$\underline{H}$), 6.59 (dd, J = 8.8, 2.4 Hz, 1H, Ar−$\underline{H}$), 6.41 (d, J = 2.4 Hz, 1H, Ar−$\underline{H}$), 4.53 (t, J = 6.5 Hz, 2H, −OC$\underline{H}_2$−), 4.05 (t, J = 6.0 Hz, 2H, −OC$\underline{H}_2$−), 3.39 (br s, 2H, −N(C$\underline{H}$)$_2$−), 2.77 (t, J = 7.2 Hz, 2H, −COC$\underline{H}_2$−), 1.97–1.81 (m, 4H, −(C$\underline{H}_2$)$_2$−), 1.69–1.26 (m, 14H, −C$_7\underline{H}_{14}$−); ^{13}C NMR (126 MHz, $CDCl_3$) δ 194.5, 190.6, 165.4, 163.8, 128.8, 115.2, 110.3, 101.2, 67.8, 67.4, 37.4, 28.4, 25.2, 19.7. ESI-MS *m/z*: 396.04 [M + H]$^+$; HRMS: calcd for $C_{20}H_{30}NO_3S_2$ [M + H]$^+$ 396.1662, found 396.1666; HPLC purity, 97.83%.

*4.5.22. 5-((4-oxochroman-7-yl)oxy)pentyl diisopropylcarbamodithioate (**15b**)*

Yield 87%; yellow oil; ^{1}H NMR (500 MHz, $CDCl_3$) δ 7.77 (dd, J = 8.8, 2.8 Hz, 1H, Ar−$\underline{H}$), 6.50 (dd, J = 8.8, 2.3 Hz, 1H, Ar−$\underline{H}$), 6.32 (d, J = 2.3 Hz, 1H, Ar−$\underline{H}$), 4.44 (dd, J = 9.1, 3.7 Hz, 2H, −OC$\underline{H}_2$−), 3.93 (t, J = 6.4 Hz, 2H, −OC$\underline{H}_2$−), 3.31 (dt, J = 14.8, 7.1 Hz, 2H, −N(C$\underline{H}$)$_2$−), 2.68 (t, J = 6.5 Hz, 2H, −COC$\underline{H}_2$−), 1.80–1.18 (m, 20H, −C$_{10}\underline{H}_{20}$−); ^{13}C NMR (126 MHz, $CDCl_3$) δ 194.7, 189.6, 164.5, 162.8, 127.8, 114.1, 109.3, 100.2, 67.1, 66.4, 48.4, 45.7, 36.4, 27.4, 24.5, 23.7, 18.7. ESI-MS *m/z*: 410.07 [M + H]$^+$; HRMS: calcd for $C_{21}H_{32}NO_3S_2$ [M + H]$^+$ 410.1818, found 410.1882; HPLC purity, 98.15%.

*4.5.23. 4-((4-oxochroman-7-yl)oxy)butyl 4-methylpiperazine-1-carbodithioate (**16a**)*

Yield 87%; yellow needles; m. p. 95–96 °C; ^{1}H NMR (500 MHz,

$CDCl_3$) δ 7.82 (d, J = 8.8 Hz, 1H, Ar−H), 6.56 (dd, J = 8.8, 2.3 Hz, 1H, Ar−H), 6.38 (d, J = 2.3 Hz, 1H, Ar−H), 4.50 (t, J = 6.4 Hz, 2H, −OCH_2−), 4.39 (br s, 2H, −$CSNCH_2$−), 4.02 (t, J = 5.8 Hz, 4H, −$CSNCH_2$−, −OCH_2−), 3.38 (t, J = 6.9 Hz, 2H, −SCH_2−), 2.74 (t, J = 6.5 Hz, 2H, −$COCH_2$−), 2.61 (br s, 4H, −$N(CH)_2$−), 2.41 (s, 3H, −NCH_3), 1.94–1.87 (m, 4H, −$(CH_2)_2$−). ^{13}C NMR (126 MHz, $CDCl_3$) δ 197.4, 190.7, 165.5, 163.9, 129.0, 115.3, 110.4, 101.3, 67.9, 67.5, 54.3, 45.4, 37.6, 36.8, 28.3, 25.5. ESI-MS m/z: 395.16 $[M + H]^+$; HRMS: calcd for $C_{19}H_{27}N_2O_3S_2$ $[M + H]^+$ 395.1458, found 395.1465; HPLC purity, 96.11%.

4.5.24. 5-((4-oxochroman-7-yl)oxy)pentyl 4-methylpiperazine-1-carbodithioate (16b)

Yield 87%; white solid; m. p. 84–86 °C; ^{1}H NMR (500 MHz, $CDCl_3$) δ 7.73 (d, J = 8.8 Hz, 1H, Ar−H), 6.47 (dd, J = 8.8, 2.3 Hz, 1H, Ar−H), 6.29 (d, J = 2.2 Hz, 1H, Ar−H), 4.41 (t, J = 6.4 Hz, 2H, −OCH_2−), 4.20 (br s, 2H, −$CSNCH_2$−), 3.89 (t, J = 6.3 Hz, 2H, −OCH_2−), 3.23 (t, J = 7.4 Hz, 2H, −SCH_2−), 2.85 (br s, 2H, −$CSNCH_2$−), 2.65 (t, J = 6.4 Hz, 2H, −$COCH_2$−), 2.55 (s, 3H, −NCH_3), 1.77–1.46 (m, 10*H*, −C_5H_{10}−); ^{13}C NMR (126 MHz, $CDCl_3$) δ 198.7, 190.7, 165.5, 163.9, 129.0, 115.3, 110.3, 101.3, 68.2, 67.5, 53.5, 37.6, 28.6, 25.5. ESI-MS m/z: 409.17 $[M + H]^+$; HRMS: calcd for $C_{20}H_{29}N_2O_3S_2$ $[M + H]^+$409.1614, found 409.1616; HPLC purity, 97.46%.

4.5.25. 4-(((4-((4-oxochroman-7-yl)oxy)butyl)thio)carbonothioyl) piperazine-1-carboxylate (17a)

Yield 87%; white solid; m. p. 85–87 °C; ^{1}H NMR (500 MHz, $CDCl_3$) δ 7.81 (d, J = 8.8 Hz, 1H, Ar−H), 6.55 (dd, J = 8.8, 2.3 Hz, 1H, Ar−H), 6.37 (d, J = 2.3 Hz, 1H, Ar−H), 4.49 (t, J = 6.4 Hz, 2H, −OCH_2−), 4.30 (br s, 2H, −$CSNCH_2$−), 4.01 (t, J = 5.8 Hz, 2H, −OCH_2−), 3.93 (br s, 2H, −$CSNCH_2$−), 3.54–3.52 (m, 4H, −$N(CH_2)_2$−), 3.38 (t, J = 6.9 Hz, 2H, −SCH_2−), 2.73 (t, J = 6.5 Hz, 2H, −$COCH_2$−), 1.93–1.86 (m, 4H, −$(CH_2)_2$−), 1.46 (s, 9H, −$(CH_3)_3$); ^{13}C NMR (126 MHz, $CDCl_3$) δ 197.6, 190.6, 165.4, 163.9, 154.6, 129.0, 115.3, 110.4, 101.3, 80.7, 67.8, 67.5, 50.8, 43.3, 37.5, 36.7, 28.5, 28.3, 25.5. ESI-MS m/z: 982.72 $[2M + Na]^+$; HRMS: calcd for $C_{23}H_{32}N_2O_5S_2Na$ $[M + Na]^+$ 503.1645, found 503.1651; HPLC purity, 98.57%.

4.5.26. 4-(((5-((4-oxochroman-7-yl)oxy)pentyl)thio)carbonothioyl) piperazine-1-carboxylate (17b)

Yield 87%; white solid; m. p. 106–107 °C; ^{1}H NMR (500 MHz, DMSO-d_6) δ 7.67 (d, J = 8.8 Hz, 1H, Ar−H), 6.62 (dd, J = 8.8, 2.3 Hz, 1H, Ar−H), 6.52 (d, J = 2.3 Hz, 1H, Ar−H), 4.49 (t, J = 6.4 Hz, 2H, −OCH_2−), 4.22 (br s, 2H, −$CSNCH_2$−), 4.03 (t, J = 6.4 Hz, 2H, −OCH_2−), 3.92 (br s, 2H, −$CSNCH_2$−), 3.45–3.43 (m, 4H, −$N(CH_2)_2$−), 3.27 (t, J = 7.3 Hz, 2H, −SCH_2−), 2.70 (t, J = 6.4 Hz, 2H, −$COCH_2$−), 1.76–1.66 (m, 4H, −$(CH_2)_2$−), 1.52–1.46 (m, 2H, −CH_2−), 1.41 (s, 9H, −$(CH_3)_3$); ^{13}C NMR (126 MHz, DMSO-d_6) δ 196.4, 190.6, 165.4, 164.0, 154.3, 128.7, 115.3, 110.5, 101.9, 80.0, 68.5, 67.7, 51.0, 49.6, 37.5, 36.6, 28.6, 28.5, 25.4. ESI-MS m/z: 495.01 $[M + H]^+$; HRMS: calcd for $C_{24}H_{34}N_2O_5S_2Na$ $[M + Na]^+$ 517.1801, found517.1890; HPLC purity, 95.01%.

4.5.27. 4-((4-oxochroman-7-yl)oxy)butyl benzyl(methyl)carbamodithioate (18a)

Yield 87%; yellow oil; ^{1}H NMR (500 MHz, DMSO-d_6) δ 7.67 (d, J = 8.8 Hz, 1H, Ar−H), 7.39–7.20 (m, 5H, Ar−H_5), 6.63 (dd, J = 8.7, 2.3 Hz, 1H, Ar−H), 6.53 (d, J = 2.4 Hz, 1H, Ar−H), 5.33 (s, 1H, −$N(CH_3)CH$−), 5.06 (s, 1H, −$N(CH_3)CH$−), 4.49 (t, J = 6.4 Hz, 2H, −OCH_2−), 4.08–4.03 (m, 2H, −OCH_2−), 3.32 (s, 3H, −$N(CH_3)CH_2$−), 3.27 (br s, 2H, −SCH_2−), 2.69 (t, J = 6.4 Hz, 2H, −$COCH_2$−), 1.82 (br s, 4H, −$(CH_2)_2$−); ^{13}C NMR (126 MHz, DMSO-d_6) δ 197.7, 190.5, 165.2, 163.9, 136.4, 129.3, 129.1, 128.6, 127.8, 127.3, 115.3, 110.5, 101.8, 68.1, 67.6, 59.0, 44.0, 37.3, 36.9, 28.1, 25.5. ESI-MS m/z: 416.06 $[M + H]^+$; HRMS: calcd for $C_{22}H_{25}NO_3S_2Na$ $[M + Na]^+$ 438.1168, found 438.1177; HPLC purity, 97.62%.

4.5.28. 5-((4-oxochroman-7-yl)oxy)pentyl benzyl(methyl)carbamodithioate (18b)

Yield 84%; yellow oil; ^{1}H NMR (500 MHz, DMSO-d_6) δ 7.67 (d, J = 8.8 Hz, 1H, Ar−H), 7.38–7.02 (m, 5H, Ar−H_5), 6.63–6.60 (m, 1H, Ar−H), 6.54 (d, J = 2.0 Hz, 1H, Ar−H), 5.33 (s, 1H, −$N(CH_3)CH$−), 5.06 (s, 1H, −$N(CH_3)CH$−), 4.49 (t, J = 6.4 Hz, 2H, −OCH_2−), 4.05–4.01 (m, 2H, −OCH_2−), 3.30–3.24 (m, 5H, −$N(CH_3)$, −SCH_2−), 2.70 (t, J = 6.4 Hz, 2H, −$COCH_2$−), 1.78–1.66 (m, 4H, −$(CH_2)_2$−), 1.55–1.46 (m, 2H, −CH_2−). ^{13}C NMR (126 MHz, DMSO-d_6) δ 197.8, 190.5, 165.3, 163.9, 136.4, 135.8, 129.3, 129.1, 128.6, 127.9, 127.3, 115.2, 110.4, 101.7, 68.4, 67.6, 58.9, 44.0, 37.3, 28.5, 25.3. ESI-MS m/z: 430.05 $[M + H]^+$; HRMS: calcd for $C_{23}H_{28}NO_3S_2$ $[M + H]^+$ 430.1505, found430.1504; HPLC purity, 96.32%.

5. Biological evaluation

5.1. In vitro inhibition of eeAChE and eqBuChE

The inhibitory activities of test compounds **6–18** against ChEs were measured by Ellman's method [29]. eeAChE, eqBuChE, acetylthiocholine iodide (ATCI), S-butylthiocholine iodide (BTCI), 5,5′-dithiobis-(2-nitrobenzoic acid) (DTNB) and reference compounds (donepezil and tacrine) were purchased from Sigma-Aldrich (St. Louis, MO, USA). The compounds were dissolved in DMSO and diluted with the buffer solution (50 mM Tris-HCl, pH = 8.0, 0.1 M NaCl, 0.02 M $MgCl_2{\cdot}6H_2O$) to yield corresponding test concentrations (DMSO < 0.01%). In each well of the plate, 160 μL of 1.5 mM DTNB, 50 μL of eeAChE (0.22 U/mL, from Electric eel) or 50 μL of eqBuChE (0.12 U/mL, from equine serum) were incubated with 10 μL of different concentrations of test compounds at 37 °C for 6 min. After this, acetylthiocholine iodide (15 mM) or S-butyrylthiocholine iodide (15 mM) as the substrate (30 μL) was added and the absorbance was measured with a wavelength of 405 nm at different time intervals (0, 60, 120, and 180 s). IC_{50} values were calculated as concentration of compound that produces 50% enzyme activity inhibition, using the Graph Pad Prism 4.03 software (San Diego, CA, USA). Results are expressed as the mean ± SD of at least three different experiments performed in triplicate.

5.2. Kinetic study of eeAChE inhibition

The kinetic study of eeAChE inhibition was carried out based on our previously reported method [24,25]. Relatively low concentrations of the substrate acetylthiocholine (0.05–0.50 mM) were reacted with eeAChE in the absence or presence of different concentrations of compound **6c** (0.05, 0.10, 0.20 μM), and the activities were measured at different times. Then, the Lineweaver-Burk reciprocal plots were constructed by plotting 1/velocity against 1/[substrate], and the plots were assessed by a weighted least-squares analysis using Graph Pad Prism 4.03 software (San Diego, CA, USA).

5.3. Molecular modeling studies

Molecular modeling simulation were carried out using the Chemical Computing Group's Molecular Operating Environment (MOE) software (Montreal, Canada, version 2015.10). The docking template structure of AChE was derived from the crystal structure of *Tc*AChE complexed with donepezil (PDB code 1EVE) and all water molecules were removed. The protein was energy minimized and 3D protonated using the structure preparation module of MOE. Ligand file for the molecular docking studies were prepared in MOE and were followed by energy optimization at a standard MMFF94 force field level, with a 0.0001 kcal/mol energy gradient convergence criterion. Then, the optimized geometry of ligand was saved in a molecular database file and docked into the active site of the protein using the MOE-Dock program. The London dG was chosen as initial scoring method and Rigid Receptor was selected as the final scoring method. The best 5 poses of

each ligand were retained and scored. The MOE's pose viewer utility was used to analyze the geometry of resulting complex.

5.4. In vitro blood-brain barrier permeation assay

In order to predict the BBB penetration of the test compounds, a parallel artificial membrane permeation assay (PAMPA) for blood-brain-barrier described by Di et al. was performed [33]. The test compound was first dissolved in DMSO and then diluted with PBS/EtOH (70:30) buffer to reach the final concentration 25 μg/mL. The filter membrane of donor microplate (PVDF membrane, pore size 0.45 mm, Millipore) was impregnated with 4 μL of PBL (Avanti Polar Lipids) in dodecane (20 mg/mL, Sigma-Aldrich). Then, 300 μL of buffer was added to corresponding acceptor well and 200 μL of diluted solution was added to each test donor well. Afterwards, the acceptor filter plate was carefully placed on the donor plate so that the coated membrane could touch both donor solution and acceptor buffer. After incubation for 18 h at 25 °C, two plates were carefully separated, and the concentrations of tested compounds in reference, acceptor and donor wells were measured using a UV plate reader (SpectraMax Plus 384, Molecular Devices). Each compound was analyzed at five wavelengths in four wells at least three independent runs, and the results were expressed as mean ± SD. P_e was calculated by the following expression: $P_e = \{-V_d V_a/[(V_d + V_a)At]\}\ln$ (1-drugacceptor/drugequilibrium), where V_d is the volume of donor well, V_a is volume in acceptor well, A is the filter area, t is the permeation time, $drug_{acceptor}$ is the absorbance obtained in the acceptor well and $drug_{equilibrium}$ is the theoretical equilibrium absorbance. A good linear correlation was obtained by plotting the experimental data against the bibliographic values: P_e (exp.) = 0.9075 P_e (bibl.) − 0.2016 (R_2 = 0.9654).

5.5. Inhibition of $A\beta_{1\text{-}42}$ self-induced aggregation

The inhibitory activities of selected compounds on self-induced $A\beta_{1\text{-}42}$ aggregation were evaluated by a Thioflavin T (ThT)-binding assay [34,35]. 1,1,1,3,3,3-hexafluoro-2-propanol (HFIP) and Thioflavin T (ThT) were purchased from TCI (Shanghai) Development. β-Amyloid$_{1\text{-}42}$ ($A\beta_{1\text{-}42}$), supplied as trifluoroacetate salt, was obtained from Royobiotech Co., Ltd (Shanghai, China). $A\beta_{1\text{-}42}$ samples were pretreated with HFIP and then resolubilized with a 50 mM phosphate buffer (pH 7.4) to give a 25 μM solution. The test compound was dissolved in DMSO in 250 μM for storage and it needed not to be diluted before use. For assays, 1 μL of test compound (25 μM, final concentration) and 9 μL of $A\beta_{1\text{-}42}$ sample were added to each well of the black plate, and the obtained mixtures were incubated in dark at room temperature for 46–48 h with no agitation.

After the incubation, 200 μL of 5 μM ThT in 50 mM glycine-NaOH buffer (pH 8.0) was added to each well, and the fluorescence was measured on a multi-mode plate reader (SpectraMax M5, Molecular Devices, Sunnyvale, CA, USA) with excitation and emission wavelengths at 446 nm and 490 nm, respectively. Each assay was run in triplicate and the solvent control was also included. The fluorescence intensities were compared and the percent inhibition due to the presence of the inhibitor was calculated by the following formula: 100 - (IF_i/IF_o*100) where IF_i and IF_o are the fluorescence intensities obtained for $A\beta_{1\text{-}42}$ in the presence and in the absence of inhibitor, respectively.

5.6. Inhibition of AChE-induced $A\beta_{1\text{-}42}$ aggregation

The inhibitory activities of selected compounds on AChE-induced $A\beta_{1\text{-}42}$ aggregation were also evaluated by the ThT assay [36,37]. $A\beta_{1\text{-}42}$ and eeAChE were purchased from Royobiotech Co., Ltd (Shanghai, China) and Sigma-Aldrich (St. Louis, MO, USA), respectively. For co-incubation experiments, aliquots of $A\beta_{1\text{-}42}$ peptide and AChE in presence or absence of the test compounds were incubated for 48 h at 37 °C. The final concentrations of Aβ (dissolved in DMSO and diluted 0.215 M sodium phosphate buffer, pH 8.0), eeAChE (dissolved in 0.215 M sodium phosphate buffer, pH 8.0) and test compounds were 200 μM, 2 μM and 100 μM, respectively. After co-incubation, 200 μL of 5 μM ThT in 50 mM glycine-NaOH buffer (pH 8.0) was added, and the percent inhibition was calculated by the method same as that of self-induced $A\beta_{1\text{–}42}$ experiment.

5.7. Cytotoxicity study of human neuroblastoma SH-SY5Y cells

The cytotoxicity of compound **6c** and donepezil on the human neuroblastoma SH-SY5Y cells was evaluated by MTT assay, following a method reported previously [38]. The SH-SY5Y cells were grown in a 1:1 mixture of Eagle's minimum essential medium (EMEM) and ham's F-12 medium supplemented with 10% fetal bovine serum (FBS) and antibiotics (100 mg/mL streptomycin and 100 U/mL penicillin) in 5% CO_2 at 37 °C. For assays, 10,000 SH-SY5Y cells per well were seeded into a clear 96-well plates and incubated with different concentrations of compound **6c** or donepezil for 24 h. Then, 20 μL of MTT was added and incubated at 37 °C for 4 h. After that, the medium was removed, and the formazan crystal formed was dissolved in 200 μL of DMSO. The absorbance at 570 nm was measured using a microculture plate reader with a reference wavelength of 630 nm. Results are expressed as the mean ± SD of three independent experiments.

5.8. In vivo studies

5.8.1. Materials and animals

Donepezil hydrochloride and Scopolamine were obtained from the Energy Chemical Co., Ltd (Shanghai, China) and SuichengPharmaceutical Co. Ltd. (Zhengzhou, China), respectively. All kunming mice weighting 18–25 g were obtained from Hunan SJA Laboratory Animal Co., Ltd. and randomly divided into corresponding groups. They were maintained under a 12 h light/dark cycle and allowed free access to tap water and standard laboratory chow. The room was maintained at temperature of 23 ± 2 °C with a relative humidity of 55 ± 5%. Compound **6c** was suspended in 0.5% carboxymethyl cellulose sodium (CMC-Na) salt solution and given via oral administration to animals. All procedures were carried out in agreement with the institutional guidelines for animal care and use and were approved by the Ethical Committee at Jiangxi University of Traditional Chinese Medicine (No. JZLLSC2018-1204).

5.8.2. Acute oral toxicity studies [24,25,39]

A total of 40 Kunming mice (half male and half female) were used to determine the acute toxicity of compound **6c**. Compound **6c** was suspended in 0.5% carboxymethyl cellulose sodium (CMC-Na) salt solution and given via oral administration to the divided experimental groups (at 0, 625, 1250 and 2500 mg/kg, n = 10 per group). After administration, animals were observed continuously for the first 4 h for any abnormal behavioral changes or deaths, then intermittently for the next 24 h, and occasionally thereafter for 14 days for the onset of any delayed effects. After 14 days, all mice were sacrificed after being anaesthetized by ether, and the possible toxic damage to heart, liver and kidneys was examined macroscopically.

5.8.3. In vivo step-down passive avoidance test [40,41]

A modification of step-down passive avoidance test was performed to assess the learning and memory in mice. A total of 48 mice were used in this test with 8 mice per group. The testing apparatus consisted of a plastic box divided into five equal cabins with grid floor made of stainless-steel bar spaced 1 cm apart. In each cabin, there is a plastic platform placed in bottom right corner. During the test, the mice received two separate trails: a training trial and a recall trial. At the beginning of the training trail, all mice were allowed to be acclimated to this environment for 5 min. Then electric currents were delivered, and each mouse was gently put on the platform. When the mouse stepped

down from the platform, intermittent electric shocks (24 V, 0.5 mA) would cause it to return to the platform. Compounds **6c** at three doses of 83.2, 41.6 and 20.8 mg/kg or donepezil at the dose of 5.0 mg/kg were orally given 1 h before the training trial. Thirty minutes later, memory impairment of the mice was induced by administering scopolamine (3 mg/kg, i.p.). The recall trial was performed after a 24 h interval, and each mouse was placed on the platform again. The latency to step down on the grid for the first time and the errors that led to a shock within 300 s were determined as the learning and memory performance.

Acknowledgement

This research work was financially supported by the Program of the National Natural Science Foundation of China [Grant No. 21807052, 81760622, 31600265, 31600275]; the Program of Natural Science Foundation of Jiangxi Province of China [Grant No. 20171BAB215064]; Project from Health and Family planning Commission of Jiangxi province [Grant No. 20173013]; the Program of Natural Science Foundation of Guangxi Zhuang Autonomous Region of China [Grant No. 2017GXNSFAA198077]; Guangxi Science and Technology Base and Special Talents Program [Grant No. AD18281032]; The program of first-class disciplines in Chinese Medicine of Jiangxi Province [Grant No. JXSYLXK-ZHYAO047].

References

[1] E.D. Roberson, L. Mucke, 100 years and counting: prospects for defeating Alzheimer's disease, Science 314 (2006) 781–784.
[2] Alzheimer's Association, Alzheimer's disease facts and figures, Alzheimer's Dement 12 (2016) 459–509.
[3] E. Scarpini, P. Scheltens, H. Feldman, Treatment of Alzheimer's disease: current status and new perspectives, Lancet Neurol. 2 (2003) 539–547.
[4] S.Y. Hung, W.M. Fu, Drug candidates in clinical trials for Alzheimer's disease, J. Biomed. Sci. 24 (2017) 47.
[5] J. Cummings, G. Lee, A. Ritter, K. Zhong, Alzheimer's disease drug development pipeline: 2018, Alzheimers Dement (N Y) 4 (2018) 195–214.
[6] G. Pepeu, M.G. Giovannini, Cholinesterase inhibitors and beyond, Curr. Alzheimer Res. 6 (2009) 86–96.
[7] M.E. Hasselmo, The role of acetylcholine in learning and memory, Curr. Opin. Neurobiol. 16 (2006) 710–715.
[8] N.I. Bohnen, M.J. Grothe, N.J. Ray, M. Muller, S.J. Teipel, Recent advances in cholinergic imaging and cognitive decline-Revisiting the cholinergic hypothesis of dementia, Curr. Geriatr. Rep. 7 (2018) 1–11.
[9] F. Mao, H. Wang, W. Ni, X. Zheng, M. Wang, K. Bao, D. Ling, X. Li, Y. Xu, H. Zhang, J. Li, Design, synthesis, and biological evaluation of orally available first-generation dual-target selective inhibitors of acetylcholinesterase (AChE) and phosphodiesterase 5 (PDE5) for the treatment of Alzheimer's disease, ACS Chem. Neurosci. 9 (2018) 328–345.
[10] L.Y. Yip, C.C. Aw, S.H. Lee, Y.S. Hong, H.C. Ku, W.H. Xu, J.M.X. Chan, E.J.Y. Cheong, K.R. Chng, A.H.Q. Ng, N. Nagarajan, R. Mahendran, Y.K. Lee, E.R. Browne, E.C.Y. Chan, The liver-gut microbiota axis modulates hepatotoxicity of tacrine in the rat, Hepatology 67 (2018) 282–295.
[11] B. Sameem, M. Saeedi, M. Mahdavi, A. Shafiee, A review on tacrine-based scaffolds as multi-target drugs (MTDLs) for Alzheimer's disease, Eur. J. Med. Chem. 128 (2017) 332–345.
[12] M. Harel, G.J. Kleywegt, R.B. Ravelli, I. Silman, J.L. Sussman, Crystal structure of an acetylcholinesterase-fasciculin complex: interaction of a three-fingered toxin from snake venom with its target, Structure 3 (1995) 1355–1366.
[13] L. Ismaili, B. Refouvelet, M. Benchekroun, S. Brogi, M. Brindisi, S. Gemma, G. Campiani, S. Filipic, D. Agbaba, G. Esteban, M. Unzeta, K. Nikolic, S. Butini, J. Marco-Contelles, Multitarget compounds bearing tacrine- and donepezil-like structural and functional motifs for the potential treatment of Alzheimer's disease, Prog. Neurobiol. 151 (2017) 4–34.
[14] A.D. Korczyn, The amyloid cascade hypothesis, Alzheimers Dement. 4 (2008) 176–178.
[15] O. Wirths, G. Multhaup, T.A. Bayer, A modified beta-amyloid hypothesis: intraneuronal accumulation of the beta-amyloid peptide–the first step of a fatal cascade, J. Neurochem. 91 (2004) 513–520.
[16] T.A. Bayer, O. Wirths, Focusing the amyloid cascade hypothesis on N-truncated Abeta peptides as drug targets against Alzheimer's disease, Acta Neuropathol. 127 (2014) 787–801.
[17] C. Reitz, Alzheimer's disease and the amyloid cascade hypothesis: a critical review, Int. J. Alzheimers. Dis. 2012 (2012) 369808.
[18] N.C. Inestrosa, S. Urra, M. Colombres, Acetylcholinesterase (AChE)–amyloid-beta-peptide complexes in Alzheimer's disease. the Wnt signaling pathway, Curr. Alzheimer Res. 1 (2004) 249–254.
[19] F.J. Munoz, N.C. Inestrosa, Neurotoxicity of acetylcholinesterase amyloid beta-peptide aggregates is dependent on the type of Abeta peptide and the AChE concentration present in the complexes, FEBS Lett. 450 (1999) 205–209.
[20] M.L. Tintas, V. Gembus, F. Alix, A. Barre, G. Coadou, L. Truong, M. Sebban, C. Papamicael, H. Oulyadi, V. Levacher, Rational design of carbamate-based dual binding site and central AChE inhibitors by a "biooxidisable" prodrug approach: Synthesis, in vitro evaluation and docking studies, Eur. J. Med. Chem. 155 (2018) 171–182.
[21] B. Liu, X. Yuan, B. Xu, H. Zhang, R. Li, X. Wang, Z. Ge, R. Li, Synthesis of novel 7-azaindole derivatives containing pyridin-3-ylmethyl dithiocarbamate moiety as potent PKM2 activators and PKM2 nucleus translocation inhibitors, Eur. J. Med. Chem. 170 (2019) 1–15.
[22] Z. Song, Y. Zhou, W. Zhang, L. Zhan, Y. Yu, Y. Chen, W. Jia, Z. Liu, J. Qian, Y. Zhang, C. Li, G. Liang, Base promoted synthesis of novel indole-dithiocarbamate compounds as potential anti-inflammatory therapeutic agents for treatment of acute lung injury, Eur. J. Med. Chem. 171 (2019) 54–65.
[23] J.Y. Yu, X.Q. Li, M.X. Wei, Synthesis and biological activities of artemisinin-piperazine-dithiocarbamate derivatives, Eur. J. Med. Chem. 169 (2019) 21–28.
[24] Q. He, J. Liu, J.S. Lan, J. Ding, Y. Sun, Y. Fang, N. Jiang, Z. Yang, L. Sun, Y. Jin, S.S. Xie, Coumarin-dithiocarbamate hybrids as novel multitarget AChE and MAO-B inhibitors against Alzheimer's disease: Design, synthesis and biological evaluation, Bioorg. Chem. 81 (2018) 512–528.
[25] N. Jiang, Q. Huang, J. Liu, N. Liang, Q. Li, Q. Li, S.S. Xie, Design, synthesis and biological evaluation of new coumarin-dithiocarbamate hybrids as multifunctional agents for the treatment of Alzheimer's disease, Eur. J. Med. Chem. 146 (2018) 287–298.
[26] A. Gaspar, M.J. Matos, J. Garrido, E. Uriarte, F. Borges, Chromone: a valid scaffold in medicinal chemistry, Chem. Rev. 114 (2014) 4960–4992.
[27] M. Singh, M. Kaur, N. Singh, O. Silakari, Exploration of multi-target potential of chromen-4-one based compounds in Alzheimer's disease: Design, synthesis and biological evaluations, Bioorg. Med. Chem. 25 (2017) 6273–6285.
[28] Q. Liu, X. Qiang, Y. Li, Z. Sang, Y. Li, Z. Tan, Y. Deng, Design, synthesis and evaluation of chromone-2-carboxamido-alkylbenzylamines as multifunctional agents for the treatment of Alzheimer's disease, Bioorg. Med. Chem. 23 (2015) 911–923.
[29] G.L. Ellman, K.D. Courtney, V. Andres Jr., R.M. Feather-Stone, A new and rapid colorimetric determination of acetylcholinesterase activity, Biochem. Pharmacol. 7 (1961) 88–95.
[30] J.L. Marco, M.C. Carreiras, Recent developments in the synthesis of acetylcholinesterase inhibitors, Mini. Rev. Med. Chem. 3 (2003) 518–524.
[31] Z. Najafi, M. Mahdavi, M. Saeedi, E. Karimpour-Razkenari, N. Edraki, M. Sharifzadeh, M. Khanavi, T. Akbarzadeh, Novel tacrine-coumarin hybrids linked to 1,2,3-triazole as anti-Alzheimer's compounds: In vitro and in vivo biological evaluation and docking study, Bioorg. Chem. 83 (2019) 303–316.
[32] K. Kingwell, Drug delivery: New targets for drug delivery across the BBB, Nat. Rev. Drug Discov. 15 (2016) 84–85.
[33] L. Di, E.H. Kerns, K. Fan, O.J. McConnell, G.T. Carter, High throughput artificial membrane permeability assay for blood-brain barrier, Eur. J. Med. Chem. 38 (2003) 223–232.
[34] M. Bartolini, C. Bertucci, M.L. Bolognesi, A. Cavalli, C. Melchiorre, V. Andrisano, Insight into the kinetic of amyloid β (1–42) peptide self-aggregation: elucidation of inhibitors' mechanism of action, ChemBioChem 8 (2007) 2152–2161.
[35] H.J. Ha, D.W. Kang, H.M. Kim, J.M. Kang, J. Ann, H.J. Hyun, J.H. Lee, S.H. Kim, H. Kim, K. Choi, H.S. Hong, Y. Kim, D.G. Jo, J. Lee, J. Lee, Discovery of an orally bioavailable benzofuran analogue that serves as a β-amyloid aggregation inhibitor for the potential treatment of Alzheimer's disease, J. Med. Chem. 61 (2018) 396–402.
[36] M. Bartolini, C. Bertucci, V. Cavrini, V. Andrisano, beta-Amyloid aggregation induced by human acetylcholinesterase: inhibition studies, Biochem. Pharmacol. 65 (2003) 407–416.
[37] L. Jalili-Baleh, H. Nadri, H. Forootanfar, A. Samzadeh-Kermani, T.T. Kucukkilinc, B. Ayazgok, M. Rahimifard, M. Baeeri, M. Doostmohammadi, L. Firoozpour, S.N.A. Bukhari, M. Abdollahi, M.R. Ganjali, S. Emami, M. Khoobi, A. Foroumadi, Novel 3-phenylcoumarin-lipoic acid conjugates as multi-functional agents for potential treatment of Alzheimer's disease, Bioorg. Chem. 79 (2018) 223–234.
[38] X. Li, H. Wang, Z. Lu, X. Zheng, W. Ni, J. Zhu, Y. Fu, F. Lian, N. Zhang, J. Li, H. Zhang, F. Mao, Development of multifunctional pyrimidinylthiourea derivatives as potential anti-alzheimer agents, J. Med. Chem. 59 (2016) 8326–8344.
[39] J.S. Lan, T. Zhang, Y. Liu, J. Yang, S.S. Xie, J. Liu, Z.Y. Miao, Y. Ding, Design, synthesis and biological activity of novel donepezil derivatives bearing N-benzyl pyridinium moiety as potent and dual binding site acetylcholinesterase inhibitors, Eur. J. Med. Chem. 133 (2017) 184–196.
[40] W. Fu, H. Wang, X. Ren, H. Yu, Y. Lei, Q. Chen, Neuroprotective effect of three caffeic acid derivatives via ameliorate oxidative stress and enhance PKA/CREB signaling pathway, Behav. Brain Res. 328 (2017) 81–86.
[41] M. Nasehi, S. Amin-Yavari, M. Ebrahimi-Ghiri, M. Torabi-Nami, M.R. Zarrindast, The dual effect of CA1 NMDA receptor modulation on ACPA-induced amnesia in step-down passive avoidance learning task, Eur. Neuropsychopharmacol. 25 (2015) 557–565.